Abstract

Fuelled by its benefits to asset management, the use of digital twin models for horizontal axis wind turbine applications is gaining increasing financial backing [11]. This thesis explores how a collection of simplistic interlinked models, governed by stochastic environmental inputs, can be applied in the context of wind turbine operational decision making. Modelling the wind turbine as a single degree-of-freedom flexible beam with a lumped mass, vibration analysis is applied to calculate the tower fatigue in terms of a damage indicator. Combining the projected damage indicator with a projection on the power extracted from the free-stream wind, asset management in terms of optimising profit is investigated. In order to propagate and manage the uncertainty characterised by the environmental conditions, Monte-Carlo sampling is introduced. In turn, the likelihood of model predictions are quantified and the confidence in the operational decisions pre-set for the environmental forecasts is enhanced. Subsequently, the interlinked models portray a digital twin framework that can provide a basis for the development of industry-standard models. Given a user-specified wind turbine, the results of this thesis investigate how the cut-out wind speed can be optimised to determine the threshold between reducing operational and maintenance costs and maximising income.

Contents

1 Introduction

1.1 Motivation

Stimulated by concerns of national policymakers on climate change, the demand for renewable energy is rapidly growing [4]. In 2018, renewable sources provided 33% of the electricity generated in the United Kingdom (UK), an increase of 3.8% from 2017. More specifically, wind energy was responsible for 51.8% of the electricity generated from renewable sources [15]. Therefore, both onshore and offshore wind is widely accepted as a means of supplying the UK's future demand for green energy.

The predominant means of harnessing wind energy is through the use of modern horizontal axis wind turbines (HAWTs). A HAWT operates on a simple principle of transforming the kinetic energy in the wind into electricity. The aerofoil shaped blades are designed to rotate subject to an aerodynamic lift force, producing a net positive torque on a rotating shaft. Resulting in the production of mechanical power that is transformed into electricity in a generator [21]. A diagram of a standard HAWT is shown in Figure 1.

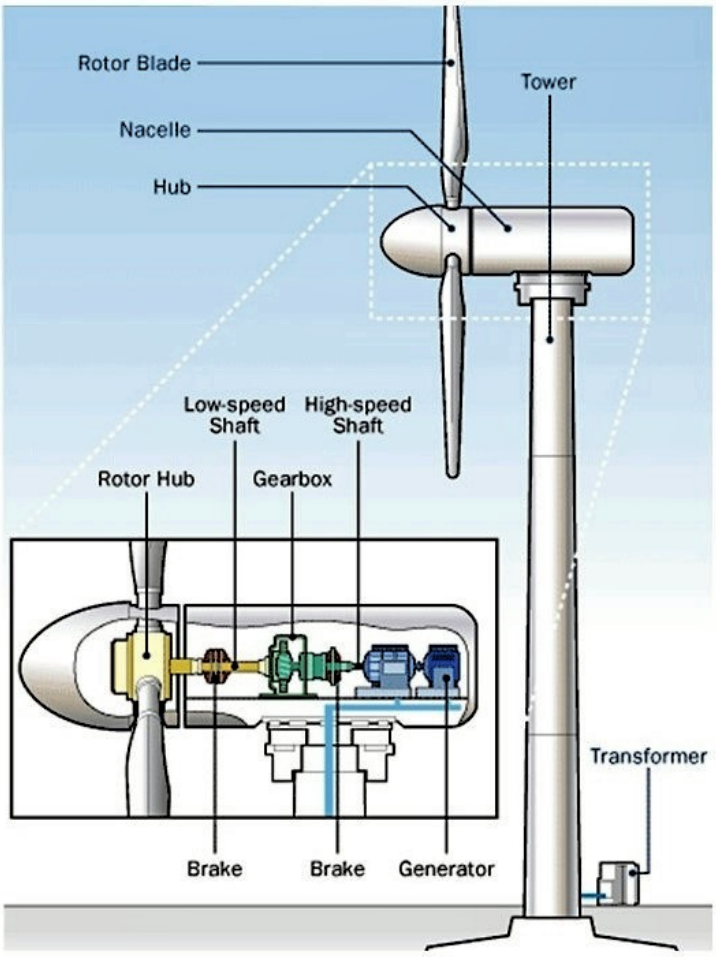

Figure 1: Schematic representation of a typical HAWT design with labelled components including a breakdown of the nacelle's internal counterparts. Figure taken from [20].

Given that the shaft is mounted horizontally, the HAWT is capable of constantly aligning or skewing itself to the direction of the free-stream wind using a yaw-adjustment mechanism. Furthermore, the importance of tower height and rotor diameter on the power output level has motivated efforts to develop larger-scale wind turbines that are capable of generating power more efficiently [18]. For example, General Electric is set to deliver the world's most powerful wind turbine, featuring a 63% capacity factor (the average power generated divided by the rated peak power) that will stand at 260 meters tall carrying a 220-meter rotor [26]. These large scale applications tend to be designed to endure harsh offshore conditions, demanding precise understanding of the dynamic behaviour and typical loads applied. Furthermore, the growth in the wind turbine tower height and rotor diameter since 1985 can be visualised graphically in [2].

Predictions on future increases in consumer demand [31] apply a constant pressure on the wind industry to reduce costs and increase revenue. Thus, introducing challenges such as actively decreasing downtime and managing turbine performance, whilst simultaneously reducing maintenance costs and extending the life of assets beyond their original design life expectancy [9]. The industry aims to alleviate these challenges using predictive models that can control and forecast component failures by advising when scheduled and unscheduled maintenance should be administered. Subsequently, mandatory turbine shutdowns that can potentially result in drastic financial losses can be avoided.

Nonetheless, the uncertainty and fluctuation of the turbine environments pose difficulties in the process of developing effective predictive computational models for design and asset management. Efficient system operation requires these predictive models to be precise. However, approximating the turbine environments render them highly sensitive to small perturbations. Therefore, developing such models has proven a challenging task thus far. For example, small changes in operational tolerances (power rating, propeller blade shape, tip-ratio speed) and environments (wind speed, energy prices, wind wake, ground effects) can lead to drastic variations in model accuracy. Without an effective method of taking these perturbations into account, current industrial practice sees the acceptance of calculation noise and error in the approximate dynamical environment. These approximation errors have led to inaccuracies in operational performance, resulting in major drawbacks regarding the reliability of the model [32].

A proposed method that has gained significant support as a possible solution is the creation of a virtual model, or in other words, a digital twin model. The digital twin is much more than just a standard numerical model: it is a virtualised 'proxy' version to its physical structure counterpart [32]. By combining a multitude of models including data sources, a rigorously tested uncertainty management framework and other models often mathematical in premise, the digital twin is able to produce a more complete virtual representation of the structure. An accepted arrangement of fused models comprised in a digital twin is outlined in Figure 2. Given that the uncertainty in the dynamical environment is being propagated accordingly, the model captures a more complete prediction on the physical system's current and future state. Thus, leading to significant advantages in operational accuracy that result in a direct increase in the reliability of operational decision making [32].

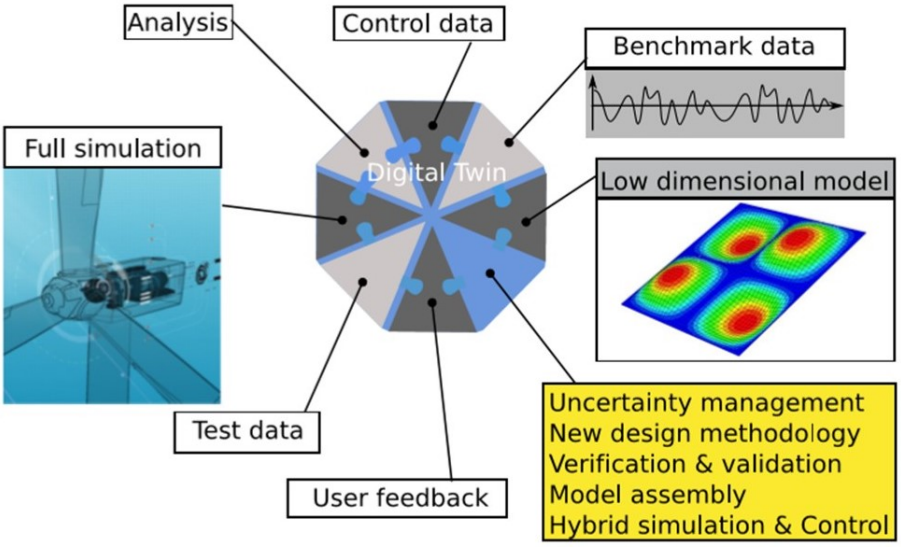

Figure 2: A typical wind turbine digital twin model fused using methods outlined in the yellow box. Figure taken from [32].

Applied correctly, the potential benefits are vast as they can bring accuracy, control and predictability to the industry. Therefore, it is highly probable that digital twin models are the next upcoming innovative method of modelling dynamical infrastructure and wind turbines in particular. As a result, support provided by sources reviewed in Section 2.1 and the industry as a whole, is the driving force behind the development of robustly validated digital twin models for a multitude of applications. Consequently, the global digital twin market was valued at $3.8bn in 2019 and is expected to reach $35.8bn by 2025 [11].

1.2 Project Aims and Objectives

Analysing the literature outlined in Sections 2.1 and 2.2, it is apparent that current digital twin models for wind turbine applications are lacking suitable uncertainty management and propagation framework. Current models tend to be deterministic and are trained to handle very specific predictable environments, conditions and structure components [32]. In this thesis attempts will be made to propagate uncertainties originating from unpredictable environments throughout a number of simplified models comprised in a digital twin framework. The propagated uncertainty will be quantified in the output of the digital twin framework, enabling comparisons between contrasting output distribution moments. When modelled appropriately, the propagated uncertainty will enhance confidence in model future predictions and subsequent decisions, leading to a more robust digital twin model. In particular, this paper aims to develop a simple framework of models investigating, with uncertainties managed and propagated accordingly throughout, how the framework can analyse damage and energy return projections. Therefore, giving the model the ability to make informed operational decisions based on projected turbine profit in user-defined timeframes. The interacting models proposed are combined to accurately demonstrate how the relationship between the digital twin and infrastructure is held throughout its life cycle, signifying its suitability in industry.

As a result, the objectives of this thesis are to:

- Identify and combine key simple models required to develop a digital twin for a wind turbine that can be used in operational decision making.
- Propagate input uncertainties originating from unpredictable environments throughout the digital twin framework and quantifying such uncertainty in the model outputs.
- Optimise operational decision making by quantitatively comparing with uncertainty quantified, contrasting outputs that project the success of the operation.

1.3 Plan of the Report

In order to achieve the aim of the thesis, a detailed digital twin framework with simplified models will be introduced in Section 3. The methodology and assumptions of the fused models describing the fidelity of the overall digital twin are outlined in Section 3.1. The model outputs will be governed by stochastic environmental models, presented in Section 3.2, that generate indicative wind speed and electricity price input data for the digital twin. Modelling the wind turbine as a single degree-of-freedom (DoF) structure, a system response model coupled with beam vibration analysis is investigated in Sections 3.3 and 3.4 respectively. Subsequently, predictive wear and system identification inter-connected models are used to evaluate the damage accumulation on the system introduced in Section 3.5.

Furthermore, in Section 3.6, a momentum model will be introduced to estimate a projection for the power extracted by the wind turbine. In association with this, income and profit indications are constructed in a model outlined in Section 3.7. These models, combined with the rest of the framework, will give the user the ability to optimise the wind turbine performance for a given forecast by minimising the accumulated damage while maximising the power extracted. A description of how the wind turbine cut-out wind speed variable is optimised in such fashion is presented in Section 6. Finally, Section 5 investigates how uncertainties in the stochastic environmental models are projected through the model as a whole and quantified in the outputs utilising a Monte-Carlo sampling method.

2 Literature Review

This section outlines the research conducted into existing knowledge and exploration on digital twin models for wind turbine applications. Attempts were made to understand the current use of digital twin models in practice, alongside relevant sub-models that are vital in building a simplistic model for operation decision making.

2.1 Digital Twins for Wind Turbines

An EPSRC Grant [32] proposes a framework for the production of robustly-validated digital twin models, which can be highly dependable in making both critical design and operational decisions in dynamical applications. The framework referenced throughout consists of three separate interlinked model stages with individual sub-stages. These include the design, uncertainty management and validation stages. More generally, they believe a digital twin should be comprised of several numerical models, that together act as a "proxy" version of the physical structure. These "twin" versions fuse multiple physical models with system performance data in order to constantly update the status of the system automatically. The scale of the model framework outlined includes a multitude of academic institutions incorporating several fully-qualified researchers, leaving the whole framework inadequate for this particular investigation. However, an insight into real-world practice with digital twins for wind turbine applications is captured.

The EPSRC Grant also raises interesting questions regarding current issues with the use of digital twin models in practice. There are significant concerns regarding the treatment of uncertainties in predictive models. Such as establishing uncertainty in input data and propagating this uncertainty appropriately throughout the model to construct confidence bounds on the model output. The proposal also highlights that digital twins of dynamical systems are very complex. Typically, multiple teams of engineers are utilised in the supervision and development of sub-models, leading to varying fidelity, assumptions and data. Subsequently, incorporating these sub-models in the overall digital twin framework while retaining the model accuracy has proven difficult.

An example of a digital twin model used in practice is the WindGEMINI model, developed by DNV.GL [9]. Used commercially, the WindGEMINI model monitors turbine integrity, performance and lifespan. This is done by utilising innovative algorithms in combination with physics-based simulation models powered by observed turbine data. For example, the turbine component temperatures are monitored, identifying trends indicative of incipient failure modes, consequently raising warnings that could potentially help prevent sudden or long-term failure. Combining physical simulation models, supervisory control and data acquisition (SCADA), the turbine component fatigue accumulation is estimated. In turn, helping the identification of faults and opportunities to replace and extend the turbine life through maintenance and other factors. This digital twin model seems to incorporate the most important factors in "digitally-

cloning" the turbine, however, there is a lack of explanation in the uncertainty management of the model. Furthermore, the model and its metadata are connected through an external provider called veracity, which may see a rise to varying fidelity in the combination of its sub-models.

In industry, there is a tendency to develop and implement digital twin models for key individual wind turbine components rather than for a whole system. Combining these component models in such a way that enables them to interact with one another simplifies the major task of developing a model for a whole system. In 2018, it was published that GE Aviation developed a digital twin for the yaw motor of the Haliade 150-6, a 6-megawatt wind turbine [25]. This paper explained that the use of virtual sensors enabled the digital twin to accurately predict the motor temperature for a multitude of conditions. As a result, the motor is used at optimal efficiencies, which lead to the avoidance of faults and shutdowns, in turn decreasing maintenance expenses. Therefore, it is concluded that coupled with digital sensors, digital twin models are able to increase the safety and sustainability of industry assets.

2.2 Evaluation of Existing Models

There are many fully operating wind turbine dynamic response models with varying complexities available. Various papers reference the FAST software as a highly accurate model incorporating more than 20 degrees of freedom (DoF). FAST is labelled as an aero-elastic computer-aided engineering tool for predicting the dynamical response for HAWTs [19]. It fuses a multitude of complex models: "aerodynamics models, hydrodynamic models for offshore structures, control and electrical system (servo) dynamics models, and structural (elastic) dynamics models". Together, these models enable coupled nonlinear aero-hydro-servo-elastic simulation in the time domain. The model is highly trusted; however, it is complex and incorporation into a digital twin framework would require extensive knowledge and experience with the software.

At the other end of the spectrum in terms of complexity, S. Adhikaria and S. Bhattacharya propose a Euler-Bernoulli beam-column model with elastic end supports that characterises the dynamic behaviour of the wind turbine tower with flexible foundations [1]. This idealised model of the turbine tower, with a lumped mass representing the mass of the nacelle and turbine blades, simplifies the process of evaluating the turbine response. Thus, enabling investigation into wind turbine tower design issues in terms of foundation parameters, leaving the model ideal for offshore conditions. Furthermore, the authors propose three turbine tower "frequency safe regions" that are modified based on periodic loading of the turbine rotary system and environmental phenomena, such as wind gusts and ocean wave loading.

Similarly, a conference paper written by A. R. Tsouroukdissian et al. [30] investigates different structural damping strategies that describe the structural integrity of a state-of-the-art multi-megawatt wind turbine. It concluded that the optimal solution from a structural, mechatronic, economical point of view, is to implement an upper toggle brace in the interior of the base of the tower. Furthermore, a typical turbine tower damper control system is presented. It is explained how the several tower lateral and longitudinal acceleration sensors are used to feedback into

the damping control for the system. As a result, critical modifications to the system damper devices by tuning the damping ratios can comfort a range of tower mode frequencies avoiding resonant-based faults.

There has been extensive research into modelling wind speed forecast prediction software due to its obvious importance to the field. With high dependence on location and atmospheric conditions, the erratic fluctuation of wind speed forecasts over time, make modelling them accurately a complex task in practice. Daily, weekly, monthly, seasonal and yearly trends all have an effect. C. Gavriluta et al. [14], H. Aksoy et al. [3] and J. F. Manwell et al. [21] all claim that the Weibull distribution captures the erratic behaviour of wind speed time series particularly well, with exception to long-term trends. Where J. F. Manwell et al. [21] examines a variety of various wind characteristics and resources that could be incorporated into a whole model, Gavriluta et al. [14] and Aksoy et al. [3] both propose similar singular first-order and second-order autoregressive (AR) models. Each type of model has its own level of complexity, suitability and accuracy.

In a similar manner, modelling the stochastic process of predicting financial markets and trends is a desirable but challenging task. In practice, due to the incorporation of random behaviour, such a process is typically modelled using a random walk formalisation. In particular, J. Masoliver et al. [22] concluded "finding a good agreement between theory and observed data", that a continuous-time random walk formalism can approximate fluctuations in the U.S. dollar–Deutsche mark future exchange. Similarly, E. F. Fama [12] assesses the theory of random walks and explains how historically, a large body of economists and statisticians adhere to the theory in the prediction of stock market prices in particular. However, a critical drawback to this particular type of model, is that it cannot be applied to any averaged market indices as the model assumes that the time between successive changes is random.

Using a time series approach, C. Su et al. [29] concluded that the changing regularity of the wind turbine failure rate can be learnt by monitoring the power index of the wind. Therefore, giving rise to a theoretical basis for preventive maintenance decisions in wind turbines. Interestingly, this approach analysed the time series data to predict the correlation between the failure rate and wind speed. However, this approach is complex as it uses spectral density, cross and autocorrelation functions. Alternatively, J. F. Manwell et al. [21] suggested a simple model that predicts when a component is deemed to fail. It does so by using a basic principle of counting the number of cyclic loads that are inflicted on the component in a given timeframe. Calculating the ratio until fatigue, a damage term is introduced. This damage term can be used to predict whether the turbine has experienced a fault and subsequently needs to undergo maintenance. This particular model would fuse predictions on turbine response and vibration with a counting algorithm to cumulatively estimate the damage inflicted, coordinating with the project scope effectively.

A. R. Jha [18] proposes two models for estimating the cost of a particular wind turbine per kilowatt-hour of energy generated. Considering both cost and efficiency, this approach allows comparisons between both several individual turbines and changes in singular turbine operating

conditions. This is highly desirable in industry as it can isolate optimal operational decisions for particular wind speed forecasts and operational states. The first model simply incorporates a turbine life-expectancy and maintenance annual running costs. Whereas, the second also factors the cost of the land, taxes, escalation and capital recovery rates in a periodic "levelising" factor that estimates both commercial and turbine costs, rendering it more complex.

2.3 Uncertainty Propagation and Management

As outlined in R. C. Smith's monograph [28], the systematic quantification of uncertainties and errors in models, simulations, and experiments is crucial in the accuracy of predictive science. Smith covers a broad but connected range of topics in uncertainty quantification. Analysis into both simple models, with singular uncertainty inputs that ideally only require the utilisation of a sampling method, and more complex models with high-dimensional parameter spaces is conducted. It is expressed that "for applications where distributions for input uncertainties have been determined either experimentally or using Bayesian type techniques, sampling methods can often be used to construct distributions for responses". However, it is also emphasised that the success of sampling methods relies on relatively fast computational simulation times, in addition to the accuracy and representation of the prior distributions for the uncertain inputs.

J. P. Murcia et al. [23] demonstrated how two methods from Smiths' monograph [28] can be fused to propagate uncertainty through an aeroelastic wind turbine model. In particular, the paper outlines how polynomial surrogate and global sensitivity analysis models can be applied to capture the global behaviour of uncertainty in a modern wind turbine under realistic inflow conditions. For example, the paper specifically investigates the energy production and lifetime fatigue loads for various components of a reference turbine, namely the DTU 10 megawatt wind turbine. The utilisation of a combination of surrogate models and global sensitivity analysis to the mean and standard deviation of each output with respect to the inflow realisations, "has a bigger impact on the total distribution of equivalent fatigue loads than the shear coefficient or yaw misalignment". Therefore, signifying its suitability to estimating the turbine fatigue load distribution and relevance to this study.

3 Digital Twin Framework

This section outlines the key components of the simplified wind turbine digital twin model required for operational decision making. The function of these components is to interact with one another in order to suggest time-dependent operational decisions analogously to that of a fully functioning, industry-standard digital twin model. The model does this by using external inputs, namely the wind speed and energy price forecasts generated for a user-specified interval, to project the wind turbine performance in terms of profit. These model components and their interactions with the inputs and outputs of the digital twin framework can be examined in Figure 3.

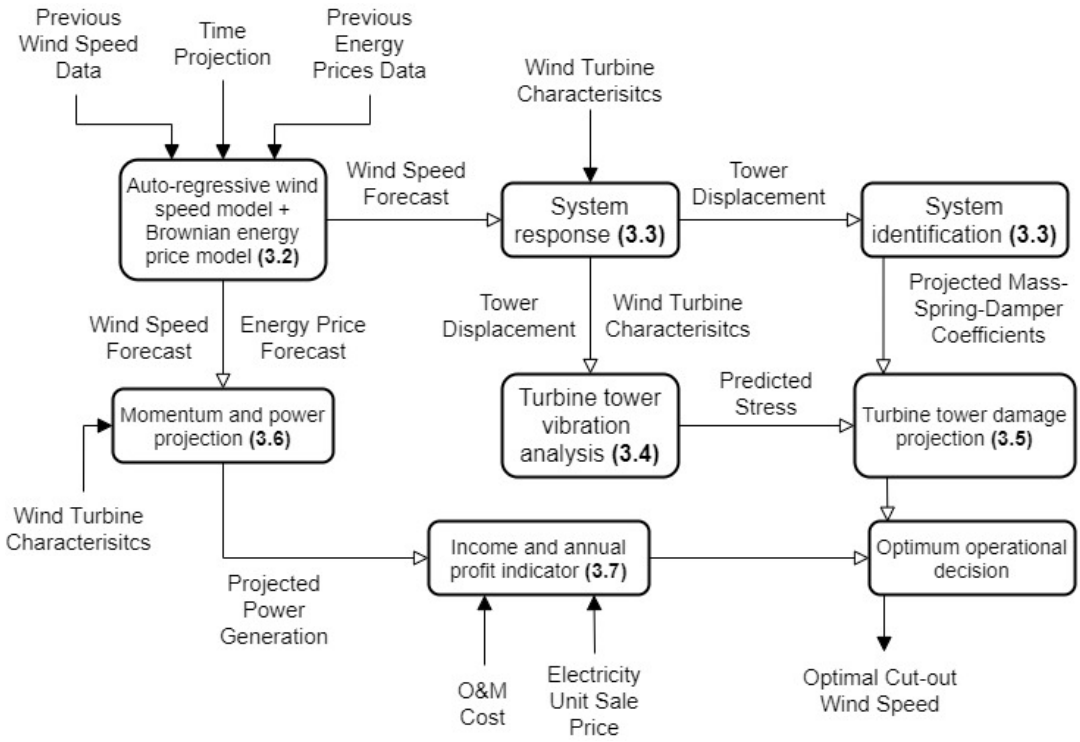

Figure 3: Block diagram showcasing the distinct components comprised in the digital twin framework and how each one interacts with one another and the input data. The component sections are referenced for each model block. Created using draw.io.

The wind turbine operational decisions can adjust which aspects of the asset operation are being prioritised, such as reducing system wear or generating power. In order to make informed, trustworthy operational decisions, input environment uncertainties are propagated through the model projecting key values that quantify turbine condition and income. In order to locate the optimal threshold between reducing system ware and increasing power generation, the operational decision of selecting the most appropriate turbine cut-out wind speed value (the value where reducing system wear is prioritised over generating power) during a user-specified time interval is investigated. In doing so, operating at this optimal value can aid in the generation of future long-term profits.

3.1 Methodology, Assumptions and Simplifications

The assumptions outlined in this subsection clearly specify the fidelity of the models used and subsequently the accuracy of the resulting outputs and conclusions. Following a similar approach outlined by S. Bhattacharya and S. Adhikaria [1], one can model the wind turbine structure as a flexible beam with a lumped mass, representing the mass of the turbine nacelle and blades. However, here the beam is modelled fixed to the ground at the 'fixed-end' and unconstrained, carrying the load applied by the lumped mass, at the 'free-end'. In order to analyse this virtual structure as a single DoF system, a vital assumption is made that the structure can only displace in the direction orthogonal to the rotor blade plane (Fore-Aft-Movement) [30]. The side view, parallel to the rotor blade plane, of this two-dimensional configuration is shown in Figure 4.

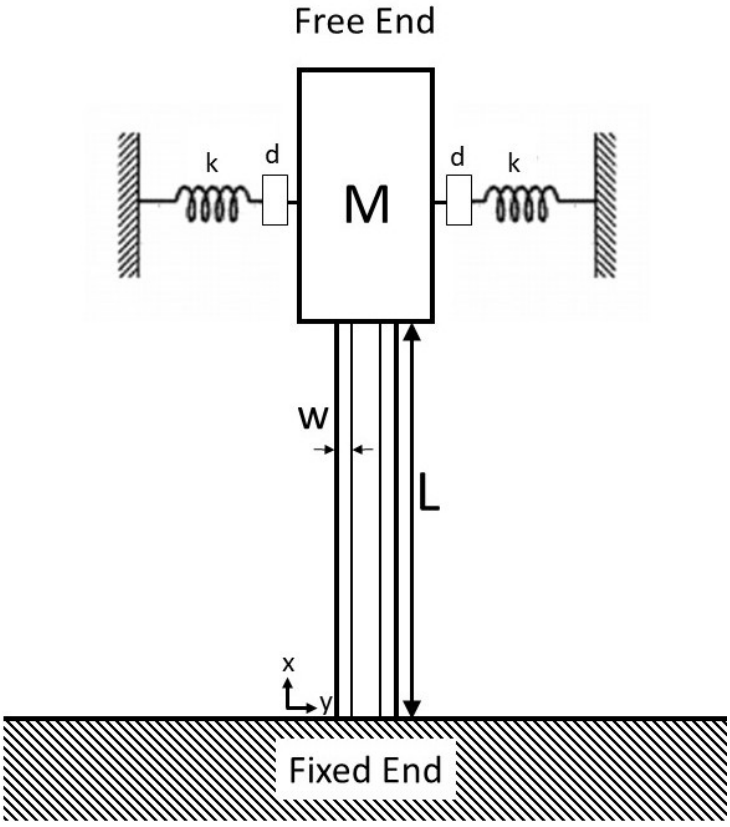

Figure 4: Side view of the system configuration consisting of a beam of length, L, and uniform thickness, w, operating as a flexible entity. The beam is fixed at one end and free, carrying lumped mass, M, at the other. The lumped mass is modelled as a forced mass-spring-damper system. It represents the higher distribution of weight at the free-end due to the significantly larger mass of the turbine blades, nacelle, gearbox and generator shown in Figure 1. In this configuration, the oncoming free-stream wind can either be directed from left-to-right or right-to-left.

It is assumed that the direction of the free-stream wind, namely the force applied to this system, can either be directed from left-to-right or right-to-left with reference to Figure 4. This directed free-stream wind is able to excite the lumped mass system similar to that of a forced mass-spring-damper system. Furthermore, modern HAWTs are able to auto-correct their configuration

enabling them to consistently face the direction of the oncoming free-stream wind. Therefore, it is assumed that given the free-stream wind speed is within the turbine cut-in and cut-out speed, power is consistently being extracted by the wind turbine.

Moreover, when the free-stream wind speed surpasses the turbine cut-out wind speed, it is assumed that the turbine undergoes a shutdown. This shutdown sees the turbine re-align itself perpendicular to the oncoming free-stream wind, thus significantly reducing the aerodynamic effects acting on the system. As a result, it is assumed that during a shut down the mass-spring-damper system is no longer excited by the free-stream wind. When the free-stream wind speed then returns within the cut-in and cut-out wind speed, the wind turbine is restarted and re-aligned parallel to the oncoming free-stream wind. In reality, this start-up is not instantaneous. To model the start-up, a delay is introduced that sees the turbine left inactive for one hour before restarting.

Controlling the surrounding wind speed is impossible. However, it is common knowledge that the greater the blade length, the higher the power extracted. This physical phenomenon has led to the ever-increasing desire to construct taller turbines with longer blades. Subsequently, it is often difficult to conduct maintenance and mitigate loads on the taller turbine towers. As a result, the digital twin framework developed focuses its attention on investigating the loads applied to a user-defined turbine tower. The analysis conducted on the projected loads applied to the tower are used in assisting to pre-set uncertainty dependent operational decisions. The parameters that characterise which specific turbine tower is to be analysed are listed in Tables 2 and 1.

The trivial aspect of designing the turbine tower in such a way that mitigates material fatigue is to ensure that the natural frequency of the tower evades the expected frequency of the system's sources of excitation. As mentioned in Section 2.2, Adhikaria and Bhattacharya propose three tower natural frequency "safe frequency zones" [1] that avoid the maximum predominant frequency of the wind, rotor frequency and double the blade passing frequency. The region of safety between the frequency of the wind and rotor, rotor and 2-times the blade passing frequency, and higher are labelled SOFT-SOFT, SOFT-STIFF and STIFF-STIFF, respectively. It is assumed that the user-defined turbine tower's natural frequency sits in one of these zones. As a result, concerns on analysing natural frequencies are mitigated.

3.2 Environmental Inputs

There are numerous environmental factors that can have a significant impact on turbine performance and component deterioration over time, each of which should be incorporated into the digital twin as an input. For this simple digital twin framework only the two key environmental factors that govern the operational decisions of the turbine are incorporated. These include predicting, with uncertainty quantified, how the future electricity price and wind speed forecasts will fluctuate in a user-specified future time-interval. However, in industry there are a number of specialist companies that provide well-developed numerical models for such applications that

can be used in place. The advantageous aspect of the digital twin enables models/data to be substituted in and out of the model, adjusting the prediction accuracy accordingly.

Accurately predicting the fluctuation in future wind speed and electricity price forecasts is a highly desirable ability for a prosperous operation of a wind turbine. An accurate prediction software can introduce the potential of pre-setting wind turbine operational decisions for uncertain, probability-dependent future events with greater confidence. Thus, providing the industry with the tools to pre-set turbine operation in crucial timeframes, where desirable wind speeds and electricity prices are categorised highly likely for a considerable length of time. This can make significant enhancements to the energy generation, improving the overall performance and profits.

As outlined in Section 2.2, the use of an autoregressive (AR) Weibull distributed scheme is appropriately adopted in the generation of accurate wind speed time series forecasts, subject to a relatively short prediction interval. In contrast to the models investigated that use a singular initial value, this model is able to process a data series of previous wind speeds as an input [13]. As a result, provided a sufficient amount of data is passed, the model is granted access to seasonal wind speed trends; improving its prediction for longer prediction intervals. The *kde* [5] MATLAB function is utilised to fit a distribution to this input data, which is then used in the AR scheme. For the simulations analysed in this thesis specifically, a monthly mean wind speed data series is passed to the model. The data series and the distribution fitted to the data series are presented in red in Figures 5a and 5b, respectively.

Beginning with the final wind speed in the input data set, v_1, the second-order AR method is used to generate the time-dependent wind speed value in an initialisation of a formalised iterative scheme [3] as shown in (1). For the second iteration onwards, the previous two values are utilised in the estimation of the next wind speed in the time series using (2). The iterative scheme is governed following,

$$v_2 = r_1 v_1 + \alpha W(5.657, 9.374), \tag{1}$$

$$v_i = \epsilon_1 v_{i-1} + \epsilon_2 v_{i-2} + \alpha W(5.657, 9.374), \tag{2}$$

where AR coefficients ϵ_1 and ϵ_2 are given by $\frac{r_1(1-r_2)}{1-r_2^2}$ and $\frac{r_2-r_1^2}{1-r_1^2}$, respectively. Furthermore, r_1 and r_2 are lag-one and lag-two autocorrelation coefficients that are equal to 0.82 and 0.688, respectively [3]. Finally, $W(5.657, 9.374)$ is a Weibull distributed random number (RN), generated using the *randdf* [16] MATLAB function, with data specific scale and shape parameter equal to 5.657 and 9.374, respectively. The values for the scale and shape parameters were estimated with 95% confidence intervals utilising the $fitwbl$ MATLAB function. This Weibull distributed RN is tuned appropriately by a coefficient α, which is a scalar value ranging between 0 and 1. For the simulations in this thesis, α is set to 0.563. This value is evaluated using a trial and error procedure where various values were tested and the resulting wind speed forecast is compared to the original input data set. The value 0.563 is found to generate a wind speed forecast that

matches the original data set most accurately. Figure 5a demonstrates a wind speed forecast generated using this iterative AR scheme model based on the monthly mean wind speed data taken from [13].

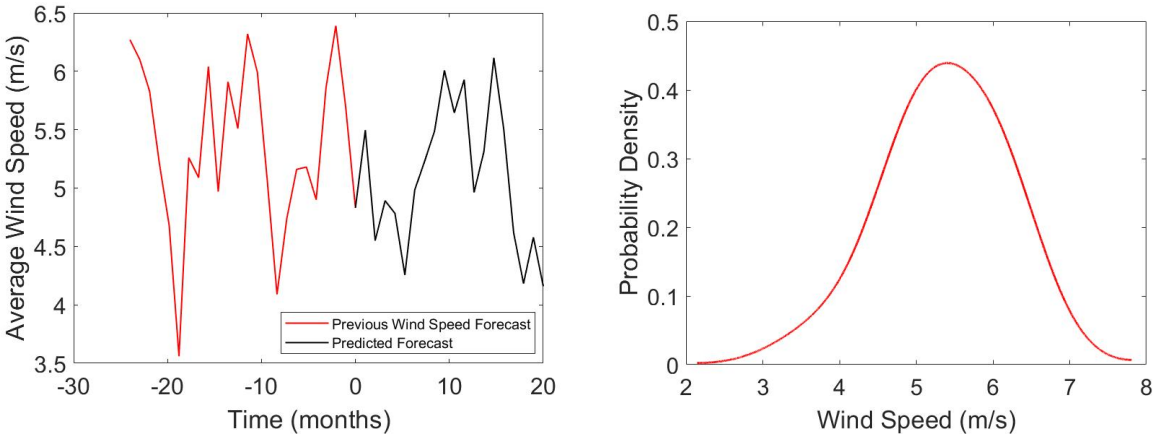

(a) Time series Prediction

(b) Previous Data Distribution

Figure 5: Figure 5a showcases the monthly mean wind speed data (red) [13] coupled with the predicted average monthly wind speed forecast generated using the AR scheme (black). Figure 5b presents the distribution fitted to the monthly mean wind speed data [13] using the *kde* [5] MATLAB function. The distribution represents a Weibull distribution with a scale and shape parameter of 5.657 and 9.3741, respectively.

As implied in Section 2.2, the use of random walk simulations dominates the role of modelling economic price movements and fluctuations. As a result, a simplistic discrete random walk model that utilises previous energy price data is implemented. Each discrete data point in the data is the monthly mean electricity supplier cost index or ESCI (GB), taken from [24]. This index is estimated using trends in network charges, wholesale prices and the charges to suppliers associated with government programs.

Identical to the wind speed model schematic, the final ESCI data point in the input data set [24], e_1, is used as the origin for the random walk simulation. Beginning at this initial value, a predicted electricity price index forecast can be assembled following an iterative formulation,

$$e_2 = e_1 + \beta D(D_\mu, D_\sigma)\sqrt{\delta T} D_\sigma, \tag{3}$$

$$e_i = e_{i-1} + \beta D(D_\mu, D_\sigma)\sqrt{\delta T} D_\sigma, \tag{4}$$

where $D(D_\mu, D_\sigma)$ is a distributed RN drawn from the input data using the *randdf* MATLAB function. The input data distribution is approximated specific to the input data set using the *kde* MATLAB function, where the mean and standard deviation are equal to $D_\mu = 102.756$ and $D_\sigma = 7.999$ respectively. In addition, e_i is the ESCI at time i and δT is the time step in the data, which is set as 1 month. Finally, β is a coefficient set as the mean of the data, D_μ, normalised by the maximum value in the data set, D_{max} ($\beta = \frac{D_\mu}{D_{max}}$). Figure 6a demonstrates an example

of an ESCI prediction (black) based on a input data series (red) [24] with distribution shown in Figure 6b.

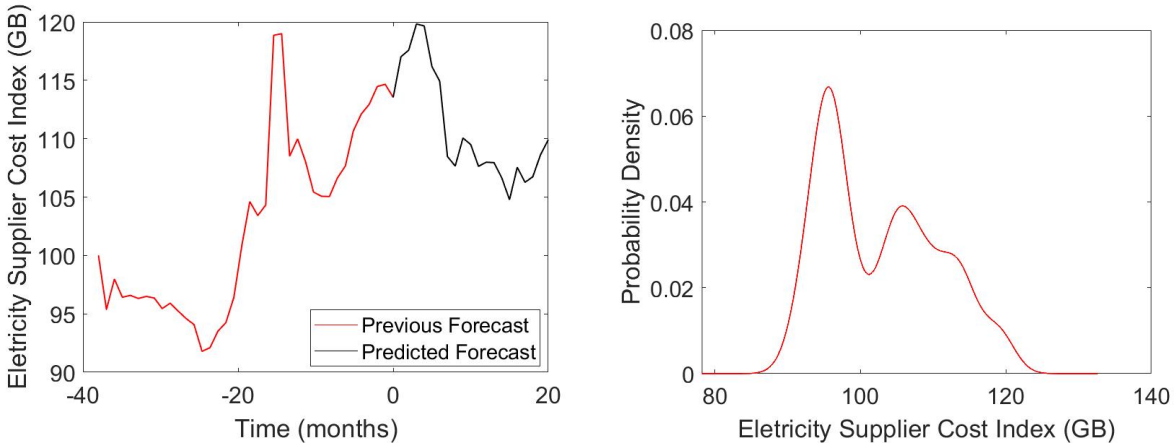

(a) Time series Prediction

(b) Previous Data Distribution

Figure 6: 6a showcases the monthly mean ESCI data (red) taken from [24] coupled with the monthly mean forecast (black) generated using the Random Walk model formalisation in (3) and (4). Furthermore, 6b showcases the distribution fitted to the monthly mean ESCI data.

Both models are implemented in such a way that allows distinct wind speed and energy price history data series to be passed, thus updating predicted trends automatically. Enabling a smooth transition when implementing with contrasting inputs for varying locations and trends.

3.3 Dynamic Response and System Identification

Accurately evaluating the system response under typical turbine loads is a primary concern for the digital twin model. If the response is inaccurately measured, predicting and assessing system and component wear and deterioration become unreliable. As mentioned previously in Section 2.2, there are many accurate models that could be implemented. However, the high complexities of these models were not suitable for the project time constraints. Therefore, the system response is modelled using a single DoF vibration system [21] describing the forced mass-spring-damper system, as shown in Figure 4. The equation of motion for this system is given by

$$m\frac{d^2z(t)}{dt^2} + d\frac{dz(t)}{dt} + kz(t) = f(t), \tag{5}$$

where $z(t)$ (m) is the displacement of the mass, M (kg). Moreover, d (kgs^{-1}) and k (kgs^{-2}) are the damper and spring constants, respectively. Finally, $f(t)$ (kgms^{-2}) is the input force applied to the system subsequent to the free-stream wind, which is governed by

$$f(t) = \frac{1}{2}\rho v(t)^2 A, \tag{6}$$

where ρ is the density of air equal to 1.225 kgm^{-3} and $v(t)$ (ms^{-1}) is the wind speed passing the propeller swept area, A (m^2).

As mentioned in Section 2.1, industry adopted digital twins for wind turbine applications are prone to utilising data taken directly from digital sensors. The metadata captures the time-dependent state of the turbine components thus updating the model states systematically. A model is introduced in conjunction with the system response that operates in a similar fashion. Using the system identification MATLAB extension [10], a nonlinear prediction model is implemented. Based on the system response, turbine operational parameters (mass, spring-like constant and damping coefficient) are fine-tuned to reproduce the system response given the exact same conditions. Fine-tuning the parameters for a multitude of conditions can see the model learn and incorporate the behaviour of the system, increasing the accuracy of the model predictions. Furthermore, this type of testing is beneficial for the design of the turbine as it fine-tunes the system parameters, indicating how the current design should or should not be regulated.

3.4 Turbine Wear and Vibration Analysis

Similar to the WindGEMINI model [9], a fatigue accumulation model is proposed in order to identify faults and opportunities to replace and extend the turbine life through scheduled and unscheduled maintenance. Manwell et al. [21] implies that there are seven types of loads experienced by an operating wind turbine that cause component fatigue, each of which should be accounted for in a fully operational digital twin model. Quantifying the component damage inflicted from these loads and identifying presumed catastrophic failures is a primary concern for the digital twin model. Manwell et al. [21] explains that cyclic loads are the most difficult type of load to mitigate and subsequently are specifically analysed in this model.

In terms of the severity of failure, the most significant component of the turbine infrastructure is the turbine tower. The excitation of the turbine tower has a significant influence on the vibration, and possibly excitation, of the resulting wind turbine components. Furthermore, as explained in Section 1.1, the scale of future wind turbine projects is increasing. Thus, demanding state-of-the-art infrastructure that can withstand wear due to harsh offshore conditions. The most crucial infrastructure element in such structures is the turbine tower. Therefore, minimising damage and vibrations inflicted on the turbine tower is a crucial task for the wind turbine operators and will be for the foreseeable future. Underestimating the importance of quantifying the turbine tower wear would be detrimental; therefore, it should arguably be investigated as early as the design stage and incorporated into the digital twin model. As a result, this particular model focuses on wear and deterioration of the wind turbine tower in contrast to any other individual component. In order to analyse when the turbine tower has experienced wear due to the cyclic loads inflicted upon it during the wind speed forecast, investigation into the transverse vibration of the beam in Figure 4 is conducted.

Following the derivation presented by D. J. Inman [17], the beam sustains a bending moment, $M(x,t)$, which is related to the deflection or deformation of the beam, $u(x,t)$. This relationship

is given by

$$M(x,t) = EI(x)\frac{\partial^2 u(x,t)}{\partial x^2}, \tag{7}$$

where E is the Young's elastic modulus material property of the beam and $I(x)$ is the cross-sectional area moment of inertia about the 'y axis' presented in Figure 4. Applying the relationship between stress, $\sigma(x,t)$, and bending moment [33],

$$\sigma(x,t) = \frac{w}{I}M(x,t), \tag{8}$$

the stress inflicted on the beam as a function of the position along the beam, x, and time, t, can be evaluated by substituting (7) into (8). This substitution leads to

$$\sigma(x,t) = wE\frac{\partial^2 u(x,t)}{\partial x^2}, \tag{9}$$

where w is the thickness of the beam as shown in Figure 4.

The beam equation with an external force applied is governed by

$$\frac{\partial^2 u(x,t)}{\partial t^2} + c\frac{\partial^4 u(x,t)}{\partial x^4} = f(t), \qquad c = \sqrt{\frac{EI}{\rho A}}, \tag{10}$$

where ρ (kgm^{-3}) is the density of the material, A (m^2) is the cross-sectional area of the beam and $f(t)$ (kgms^{-2}) is the external force applied on the flexible beam entity subject to the wind speed forecast governed by (6).

Solving for $u(x,t)$ subject to four boundary and two initial conditions using the separation of variables method, it is possible to decompose the deflection of the beam in terms of its spatial (or mode shape) and time components [17]. That is,

$$u(x,t) = X_n(x)T_n(t). \tag{11}$$

Inman [17] showed for clamped and free end boundary conditions, the mode shape is

$$X_n(x) = \cosh(\beta_n x) - \cos(\beta_n x) - \sigma_n(\sinh(\beta_n x) + \sin(\beta_n x)), \tag{12}$$

where β_n is the natural frequency and σ_n is a coefficient dependent on the mode shape.

Assuming that the beam only vibrates in its first mode of vibration, we have $\beta_1 L = 1.8751$ and $\sigma_1 = 0.7341$ [17], where L is the length of the beam as shown in Figure 4. In other words, we assume the wind speed forecast will never inflict a periodic forcing that is sufficiently significant to force the beam to vibrate in its second mode of vibration or higher. Thus, using the appropriate values for β_n and σ_n the deformation of the beam is given by

$$u(x,t) = z(t)\left[\cosh(\beta_1 x) - \cos(\beta_1 x) - \sigma_1(\sinh(\beta_1 x) + \sin(\beta_1 x))\right], \tag{13}$$

where $z(t)$ is the displacement returned from the output of the mass-spring-damper model outlined in Section 3.3.

An expression for the stress along the beam can be evaluated by differentiating (13) twice with respect to x and substituting the resulting expression into (9). For all discrete time points from the wind speed time series forecast, this expression is given by

$$\sigma(x,t) = wEz(t)\beta_1^2 \left[\cosh(\beta_1 x) + \cos(\beta_1 x) - \sigma_1(\sinh(\beta_1 x) + \sin(\beta_1 x)\right]. \tag{14}$$

For each point along the beam, time-dependent stress is applied. Identifying the different cyclic loads and counting the frequency of each individual cyclic load amplitude will allow us to quantify the damage inflicted during a specific wind speed time series. The cyclic load curve for the maximum stress point, the fixed end or root of the beam, is shown in Figure 7a.

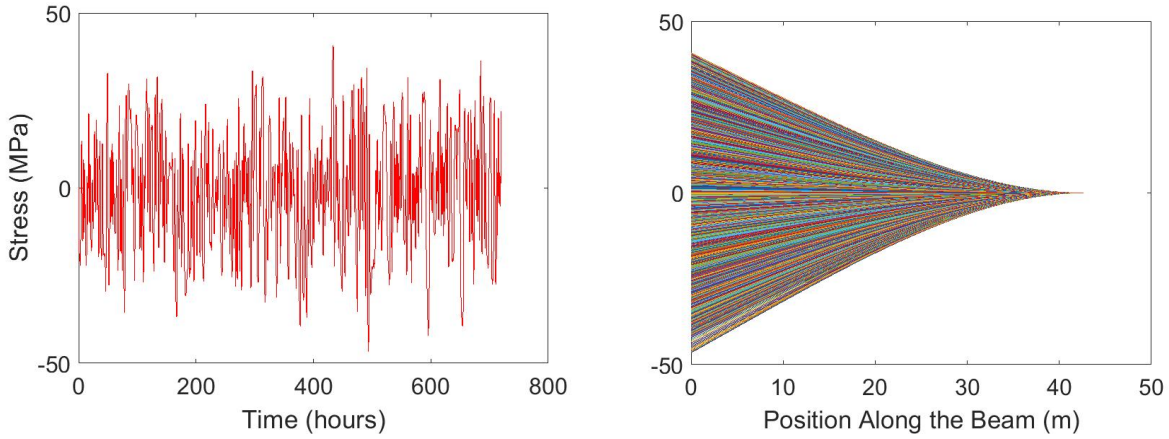

(a) Maximum stress Vs. time

(b) Stress range Vs. position

Figure 7: The stress applied to the beam during a single month, hourly-discrete, wind speed forecast. In particular, Figure 7b shows the stress profile of the beam for the different discrete time points (contrasting colours) and Figure 7a shows how the cyclic loading of the maximum stress range, at the root of the beam ($x = 0$), varies with time. The turbine parameters passed for this simulation are listed in Table 2.

3.5 Turbine Damage Indicator

The damage indicator is a dimensionless value that overcompensates the quantification of the material fatigue subsequent to cyclic loading. Coupled with accurate scheduled and unscheduled maintenance data, this indicator is able to approximate the cost of maintenance per unit time for a particular wind speed forecast. As shown in Figure 3, this has a significant impact on prioritising a particular operational decision for specific wind speed and ESCI forecasts.

In order to evaluate the damage indicator, D, based on the turbine stress prediction, a cumulative count of the number of cycles applied at each stress amplitude is normalised by the number of cycles the component material can withstand at that amplitude. That is, the ratio between the number of cycles applied, n, and the number of cycles the component can withstand before

failure, N, for each stress amplitude is cumulatively summed for all stress amplitudes [21]. Initially, n is evaluated using a cycle counting algorithm. For the analysis conducted in this thesis, the inbuilt $rainflow$ MATLAB function is the specific algorithm utilised for its simple usability. Furthermore, the value for N for each individual stress range is similar to that of a material-specific property that can be approximated by conducting experiments on the particular material used. For the simulations investigated in this thesis, the values for N for various stress amplitudes are listed in Table 1 and are taken from [27]. Hence, the total component damage is given by,

$$D = \sum_{i=1}^{M} \frac{n_i}{N_i} \leq 1,$$

where n_i is the number of cycles with a stress amplitude i and N_i is the number of cycles for failure at stress amplitude i. The closer the damage term is to 1, the higher the fatigue of the turbine component and the more serious the concern of sending out a maintenance team is. As explained in Section 4 of J.F Manwell's book [21], there are 3 types of operating conditions that result in significant cyclic loads that are accounted for in the damage term. These include [21]:

- Normal operating conditions: the turbine is operating between the cut-in and cut-out wind speeds and cyclic load magnitude is a function of the wind speed.
- Non-operating state: the turbine is currently not operating i.e., during maintenance or outside of the cut-in cut-out wind speed range.
- Normal or emergency start-up/shut down procedures: these induce transient loading which usually is more probable to cause component fatigue.

As mentioned in Section 3.1, when the free-stream wind speed surpasses the cut-out wind speed, the turbine shuts down by aligning itself perpendicular to the free-stream wind. When this happens, significant transient loads applied on the component are significantly reduced. Furthermore, as a result of the assumption that the mass-spring-damper is no longer excited, during a shutdown or a non-operating state no damage is being accumulated ($D_i = 0$). Therefore, during a specific wind speed forecast, scheduling more shutdowns by adjusting the turbine cut-out wind speed preserves the turbine by avoiding damage accumulation. Thus, minimising maintenance expenditure but adversely failing to benefit from greater power generation and profits on wind energy harvesting.

Assuming that for periodic increments in the damage term, scheduled maintenance is conducted subject to an appropriate cost value. Using the damage indicator, projected maintenance frequency can be estimated and used to scale the turbine maintenance cost value. Moreover, as the material fatigue accumulates and the damage indicator increases, more costly maintenance will need to be conducted more frequently as smaller increments in the damage indicator are more significant as its value increases.

3.6 Momentum Model and Extracted Power

The configuration of the turbine can have a direct effect on how much power will be generated for a particular wind speed forecast. The wind speed, power coefficient and area swept by the propellers are the three main factors when estimating the power generated during a particular timeframe. In fact, the power generated is proportional to the length of the propeller (radius of the area swept) squared and the free-stream wind speed cubed. However, only a subset of the wind speed forecast is extracted and converted into mechanical power and then into electricity. The region of the functional wind speed is centred between a cut-in and cut-out wind speed. Outside of this region, the turbine is shut down by aligning itself perpendicular to the oncoming free-stream wind and no power is being extracted. The relationship between wind speed and power extracted can be visualised in Figure 8.

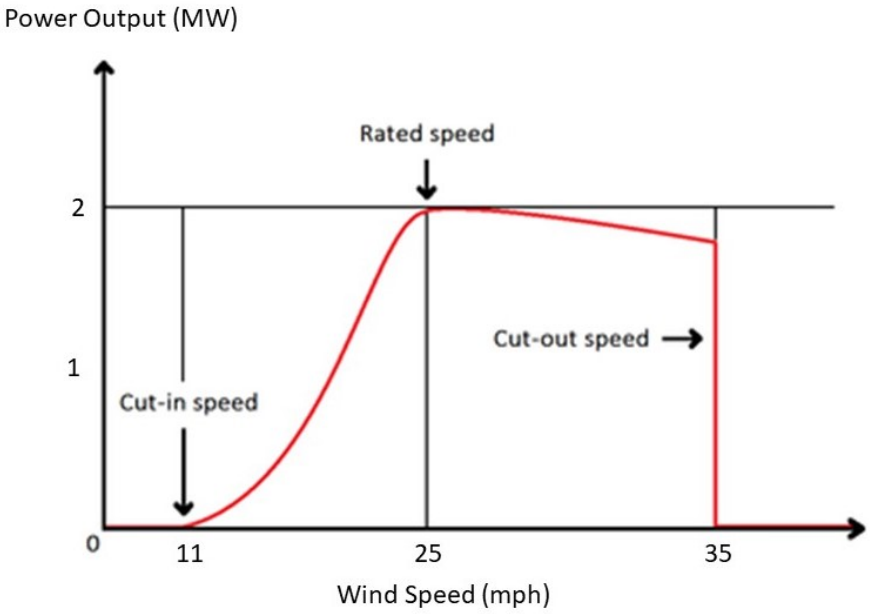

Figure 8: Power curve for a 2-MW wind turbine as listed in Appendix B. Figure taken and adapted from [6].

The power extracted by the wind turbine is the defining factor when comparing individual turbine performance and significance. In order to evaluate the power extracted from the wind speed forecast, a momentum model is proposed that is dependent on the turbine cut-in and cut-out wind speed. The hourly mean power generated (W) is given by [21],

$$P = \frac{1}{2}\rho A v^3 C_p, \tag{15}$$

where $A = \pi r^2$ is the area swept (m^2) by the turbine propellers of length r, v is the hourly mean wind speed (ms^{-1}) and C_p is a dimensionless constant called the power coefficient that is unique to each wind turbine. It has been proven that the theoretical maximum value of C_p in all cases is 0.5926 [21].

3.7 Income and Projected Profit Indicator

The power extracted by the turbine in a given time interval can be utilised in projecting the turbines short-term and long-term profit. The digital twin model will use the damage indicator, extracted power projection, income and profit figures to decide which specific operational decision should be utilised during a user-specified time interval. Specifically, this subsection outlines how both the turbine income and profit indicators are evaluated. However, the values of these elaborate estimations will remain indicative due to an insufficient amount of reliable accumulated data.

A model is developed using inspiration taken from the models outlined by A. R. Jha [18] mentioned in Section 2.2. This model is used in the digital twin framework to project the income generated by the wind turbine during a particular wind speed forecast. It does so by transforming the power prediction, estimated using (15), into a value that quantifies the projected income per hour. This transformation is estimated using the general electricity unit sale price, which is scaled in a surge or decline type modification based on the current index of the ESCI forecast. The governing expression for evaluating the projected income, PI (£/h), follows

$$PI = \frac{e_j}{100} \times U_{ep} \times P, \tag{16}$$

where e_j is the ESCI price for month j, U_{ep} is the unit electricity sale price (£/kWh) and P is the power extracted by the turbine (kW). In order to evaluate the income for a time interval that pans across multiple months, PI is calculated cumulatively for each month, j.

For instance, assuming the general electricity unit price is 0.15 £/kWh and the turbine has a projected power output of 0.5 MW, the projected income is £75 per hour. Furthermore, assuming the current ESCI is 112.5 GB, the projected income will be scaled up by 1.125, leaving a projected earning of £84.38 per hour.

Subsequently, a value for the wind turbine's projected profit per hour can be estimated using the following equation,

$$PP = PI - P \times O\&M, \tag{17}$$

where PP, PI and $O\&M$ are the projected profit (£/h), income (£/h) and operation and scheduled maintenance cost (£/kWh) respectively.

The digital twin model's sole focus was to harness the ability to suggest optimal operational decisions based on a wind speed and energy price forecast. Therefore, in contrast to the models outlined by A. R. Jha [18], this model ignores initial procurement costs for the wind turbine equipment, construction and installation labour. Such estimations would add uncertainty to the model predictions and are not a decisive element in suggesting an optimal operational decision. Thus, a fixated concern is applied to the wind turbine operation income and profits only.

4 Model Behaviour with Parameters

The digital twin framework is a combination of models interacting with a multitude of parameters, as shown in Figure 3. It is vital that users of the model have access to precise values for these parameters, either by virtue of substantial systematic testing or the use of 'digital sensors' as explained in Section 2.1. In the case of this thesis, precise turbine-dependent values for the material, environmental, operational parameters and more, are unavailable. Therefore, indicative parameter values are used in the analysis of the individual model components and results. This section outlines all the parameter values used in the simulations outlined in this thesis and explores the model behaviour while a specific subset of these parameters is varied.

4.1 Model Parameter Values

The digital twin framework incorporates three classes of parameters. These include wind turbine configuration, component material property and input and simulation parameters. All of which, inclusive of the respective simulation values, are listed in Table 2. Both the component material property parameters, taken from [27], and the wind turbine characteristic parameters, listed in Appendix B, remain constant throughout the simulations conducted in this thesis. Although, the digital twin model is constructed in a way that allows such turbine and component-specific parameters to be varied by simply adjusting the model inputs. As a result, user-experimentation with various turbines, turbine location and turbine tower materials is viable. Coupled with a planned procedure, optimal turbine location and tower material can be selected regarding projected profit values. This further demonstrates the benefits of developing digital twin models and connecting them to the asset as early as the design stage of a wind turbine/farm.

As mentioned previously in Section 3.5, the damage indicator, D, can be evaluated by dividing the ratio of cycles applied, n, by the number of cycles the component can withstand before failure, N. Subsequent to counting the stress cycles applied using the $rainflow$ MATLAB algorithm, the digital twin model requires material-specific data to compare and categorise the amplitude of these stress cycles to estimate both n_i and N_i. Typically, the turbine tower is constructed using durable tapered, tubular steel [2]. Therefore, experimental data from J. Schijve's book on a SAE 4130 test steel [27] examining the maximum number of cycles, N_i, for particular test stress magnitudes, i, is noted in Table 1 and used indicative of actual turbine tower data. However, accurate simulation results require data taken directly from experiments conducted on testing the actual material used in the construction of the turbine tower in question.

In conjunction to the wind turbine configuration parameters listed in Appendix B, indicative values for the turbine operational (mass-spring-damper system) parameters are also required. Although, in contrast to the configuration parameters, evaluating accurate values for the turbine operational parameters through rigours testing is significantly more complex. Physically adopting a procedure for testing such properties requires a more methodical approach that uses real-time data from the asset actuators and sensors. As mentioned in Section 3.3, in industry,

such systems are able to feed actual data measured from the asset itself back into the digital twin; therefore, fine-tuning operational parameters and its predictions systematically. A benefit to adopting a state-of-the-art digital twin model as early as the design stage of assets is that the user is able to experiment with various operational parameter configurations. Each configuration will require a unique system structural design resulting in unique tower dynamics. Examples of the various tower structural designs that could potentially be adopted are investigated in [30].

For the simulations conducted in this thesis, the value of the turbine lumped mass carrying the nacelle and blades, M, is taken from [7] and listed in Table 2. Moreover, given that the natural frequency of the mass-spring-damper system is governed by $\sqrt{\frac{k}{M}}$ and that the weighted natural frequency of the beam is derived by D. J. Inman [17], $\beta_1 L = 1.8751$, one can evaluate the indicative value for the tower spring constant following,

$$k = (\beta_1 L)^2 M = 1.8751^2 M. \tag{18}$$

Finally, the turbine tower damper parameter, d, is governed by the damping ratio, ζ, which is linked to M and k as follows,

$$\zeta = \frac{d}{2\sqrt{kM}}. \tag{19}$$

Acknowledging the tower flexibility, an indicative damping ratio value is chosen to equal 0.8 and the resulting values for the turbine operational parameters are listed in Table 2.

Turbine Tower Fatigue Measurement Data	
Stress Range σ_r (MPa)	Number of Cycles Before Failure N
670	1
618	50
567	100
515	300
464	700
412	1,500
361	4,000
309	15,000
258	5×10^4
206	3×10^5
155	1×10^6
103	2×10^7
52	1×10^9
0	1×10^9

Table 1: S-N curve data for SAE 4130 steel taken from [27]. This data is used to categorise the stress cycles applied by pairing them to the appropriate stress range, σ_r, returning the maximum number of cycles the specific material can withstand, N.

Symbol	Parameter	Value
Component Material Properties		
E	Young's Elastic Modulus	205 GPa
Y_s	Yield Strength	435 MPa
U_{ts}	Ultimate Tensile Strength	670 MPa
Wind Turbine Configuration		
L	Tower Height	42.672 m
w	Tower Wall Thickness	0.25 m
r	Blade Length	30.48 m
C_{in}	Cut-in Wind Speed	4.92 ms^{-1}
C_{out}	Cut-out Wind Speed	15.65 ms^{-1}
C_p	Turbine Power Coefficient	0.4
σ_1	Mode Shape Coefficient	0.7341
β_1	Tower Natural Frequency	0.0439
Input Data and Simulation Values		
μ_v, σ_v	Mean and standard deviation of the wind speed distribution	5.36, 0.71 ms^{-1}
μ_e, σ_e	Mean and standard deviation of the ESCI distribution	102.76, 8.00 GB
M	Wind Turbine Nacelle and Blades Mass	83,000 kg
k	Wind Turbine Tower Spring Constant	291830 ks^{-2}
d	Wind Turbine Tower Damper	249010 kg^{-1}
ρ	Density of Air	1.225 kgm^{-3}
r_1, r_2	Lag-one, Lag-two Autocorrelation Coefficients	0.82, 0.688

Table 2: Symbol, parameter names and values for the digital twin framework parameters. The parameter values appear in Sections 3.2, 3.4, 4, 5 and 6. The wind turbine configuration parameters where taken and adjusted from Appendix B.

4.2 Experimentation with Simulation Parameters

Understanding how the model interacts with its parameters and input data is vital in investigating the model validity. In this subsection, the fluctuation of simulation outputs is captured and discussed as a subset of the model parameters presented in Table 2 are varied. To begin with, the turbine response to variations in the means and standard deviations of the wind speed and ESCI input data (μ_v, σ_v and μ_c, σ_c) is quantified. As a result, users of the model will obtain a perception of how particular changes in forecasts will affect the resulting projected profit value.

The simulation results for the varying means and standard deviations are listed in Table 3. Analysing these results, it is apparent that variations in the moments of both the wind speed and ESCI input data act as a linear scaling for the projected income of the turbine. Moreover, analysing Table 3a, the damage indicator seems to grow exponentially for a linear increase in the moments of the wind speed input data. This exponential relationship is expected given that the higher the stress applied to the component, the more rapidly the damage indicator increases. Although, this trend only continues until the input data wind speed moments approach that of the turbine cut-out wind speed, where the damage increase is conserved as the turbine is shut down. Furthermore, Figure 9 showcases the wind turbine tower displacement for a subset of the variations in the hourly-mean input wind speed data. The significant increase in the

magnitude of displacement is clear as the wind speed, and therefore, the force applied to the system increases.

Mean and standard deviation of the wind speed input data (ms^{-1})	Income per hour (£/h)	Damage indicator, D
$\mu_v = 3.75$, $\sigma_v = 0.50$	0.62	3.91×10^{-5}
$\mu_v = 4.29$, $\sigma_v = 0.57$	4.42	3.96×10^{-5}
$\mu_v = 5.36$, $\sigma_v = 0.71$	16.90	4.32×10^{-5}
$\mu_v = 6.70$, $\sigma_v = 0.89$	39.69	7.88×10^{-5}
$\mu_v = 8.04$, $\sigma_v = 1.07$	73.53	3.15×10^{-4}
$\mu_v = 9.38$, $\sigma_v = 1.25$	101.63	0.0011
$\mu_v = 10.72$, $\sigma_v = 1.43$	127.23	0.0022
$\mu_v = 12.06$, $\sigma_v = 1.61$	117.03	0.0026

(a) Income per hour and damage indicator for varying wind speed input data.

Mean and standard deviation of ESCI input data (GB)	Income per hour (£/h)
$\mu_e = 70.07$, $\sigma_e = 6.00$	16.20
$\mu_e = 82.20$, $\sigma_e = 6.40$	17.52
$\mu_e = 102.76$, $\sigma_e = 8.00$	20.64
$\mu_e = 123.30$, $\sigma_e = 9.60$	25.35
$\mu_e = 154.13$, $\sigma_e = 12.00$	31.36
$\mu_e = 179.82$, $\sigma_e = 14.00$	36.73

(b) Income per hour for varying ESCI input data.

Table 3: Results of varying the means and standard deviations of the wind speed and ESCI input data listed in Tables 3a and 3b, respectively.

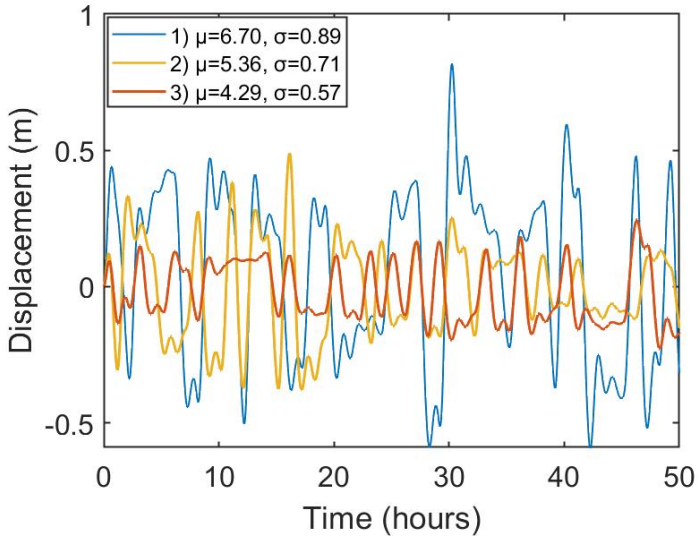

Figure 9: The resulting hourly-mean displacements for three different input wind speeds taken from Table 3a.

Another important model aspect to investigate is how changes in the tower's natural frequency affects the resulting damage indicator. Adjustments in the natural frequency of structures is often associated with increases in the component fatigue and damage or adjustments in the structure's dampers. Given the tall, slender, and flexible nature of the wind turbine structure, such adjustments in the natural frequency is common. Therefore, analysis on how the resulting variation in the turbine operational parameters for adjustments in the weighted natural frequency is conducted and the results are listed in Table 4.

Weighted Natural Frequency, $\beta_1 L$	Tower Spring Constant, k	Tower Damping Coefficient, d	Damage Indicator, D
1	83000	132800	8.56×10^{-4}
1.1429	108420	151780	3.42×10^{-4}
1.2857	137200	170740	1.61×10^{-4}
1.4286	169390	189720	8.74×10^{-5}
1.5714	204950	208680	5.80×10^{-5}
1.7143	243920	227660	4.83×10^{-5}
1.8751	291830	249010	4.32×10^{-5}
2	332000	265600	4.12×10^{-5}

Table 4: Resulting values for the turbine operational parameters and damage indicator (k, d and M) for adjustments in the weighted natural frequency, $\beta_1 L$, while M is kept constant at 83,000 kg.

Observing the results in Table 4, it is apparent that the model outlined in Section 3.5 manages to capture the general relationship between the natural frequency and the turbine damage. As outlined by A. Tsouroukdissian et al. [30], this relationship implies that taller turbines and therefore lower natural frequencies can near damaging resonant frequencies, which significantly increases the fatigue accumulation due to cyclic resonant loading. Furthermore, it is also apparent that greater spring constant, tower damping, natural frequency and smaller turbine tower height all act in decreasing the cyclic loading damage inflicted upon the tower. The ideal combination of such asset aspects can enable the design and construction of taller turbines with minimal increases in cyclic loading fatigue. However, in doing so, such refurbished designs can result in infeasible economic challenges as explained by A. Tsouroukdissian et al. [30].

In practice, for fully functional digital twin models with precise data acquired from rigours testing and asset sensors, fitting expressions to such trends analysed in this subsection are beneficial. They are able to assist in quantifying metrics that can be used in the predictive models to test for outliers in the predicted outputs and act as a validation to the model. As implied in the EPSRC Grant Proposal [32], validating the predictions of the models is a key stage in developing a robustly validated digital twin.

5 Uncertainty Propagation and Management

As explained throughout [28], there are four sources of uncertainties and errors in the general model. These include input uncertainties, model errors, numerical errors, and uncertainties in measurements. An industry-standard digital twin model will typically account for each of these sources of uncertainty, demonstrating the industry's difficulty in adopting them. To do so, generally a rigorously tested framework needs to be put in place that utilises a systematic methodology: incorporating uncertainty, quantifying the model quality by incorporating evidence from data and developing metrics that can measure the agreement between model prediction and empirical data. Therefore, ensuring the model uncertainties are propagated and validated to a certain standard, one can qualify them to be used in performance assessment and design decisions. This section presents the methodology utilised to manage and propagate the uncertainties in the inputs throughout the combined framework of models, quantifying them in the outputs. This process follows the diagram of the combined system showcased in Figure 3.

5.1 Uncertainty Propagation

As outlined in Section 2.3, for applications that only contain aleatory uncertainties (that is, the uncertainty is characterised by a distribution) and have a relatively quick simulation time, sampling methods are an effective approach of propagating the respective uncertainty. Namely, the Monte-Carlo (MC) method is a widely accepted sampling method that is based on the idea of the central limit theorem explained in Appendix A. The method works by repeatedly simulating the stochastic model in question, capturing the deviation of the model results, thus allowing statistical analysis to be performed. The accuracy of the statistical analysis is dependent on how many times the model is simulated, or equivalently, how many MC samples are used, N_{MC}. Experimenting with the running time of the model developed, the *tic* and *toc* MATLAB commands estimate a simulation time of 34.397 seconds. Therefore, signifying the feasibility of simulating with a relatively large MC sample size, $30 < N_{MC} < 10000$.

Simulating the environmental input models in Section 3.2 using the MC method with $N_{MC} = 1000$, the digital twin input uncertainties can be quantified through the construction of confidence intervals. That is, the interval of each data point (range of values from the variation between the distinct MC samples at a single time point, see Figure 10) has an associated confidence level that the true data point is located within the proposed range. In particular, 95% confidence intervals are estimated by multiplying the standard deviation of the interval by 1.96. This is due to the fact that it is assumed the central limit theorem holds approximately and the sample distribution, $\bar{X}$, represents the normal distribution. Therefore, 95% of the probability density lies within the range $\mu_{\bar{X}} \pm 1.96\sigma^2_{\bar{X}}$. Figure 10 shows the MC method simulation results for the environmental inputs.

The uncertainty in the environmental input models is propagated through the whole digital twin framework by simulating for all N_{MC} environmental input data series. The resulting stochastic

digital twin model outputs, namely the projected damage indicator and the average power generated are shown in Figures 11a and 11b, respectively.

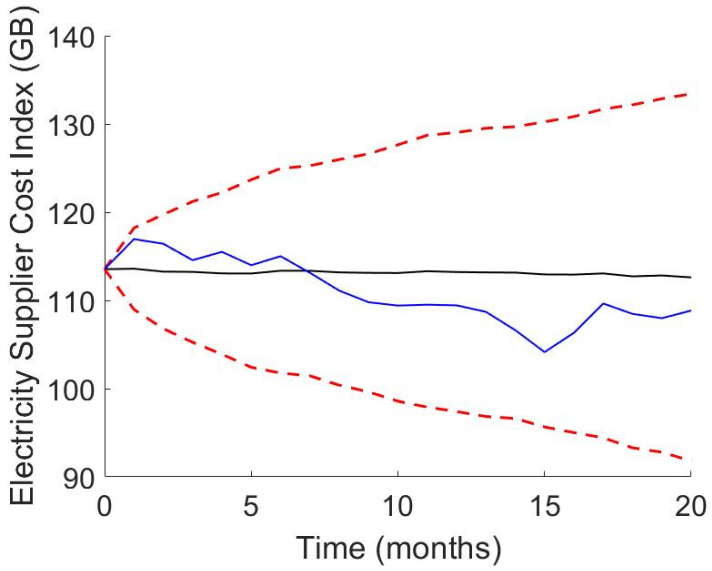

(a) MC ESCI forecast simulation with monthly data points

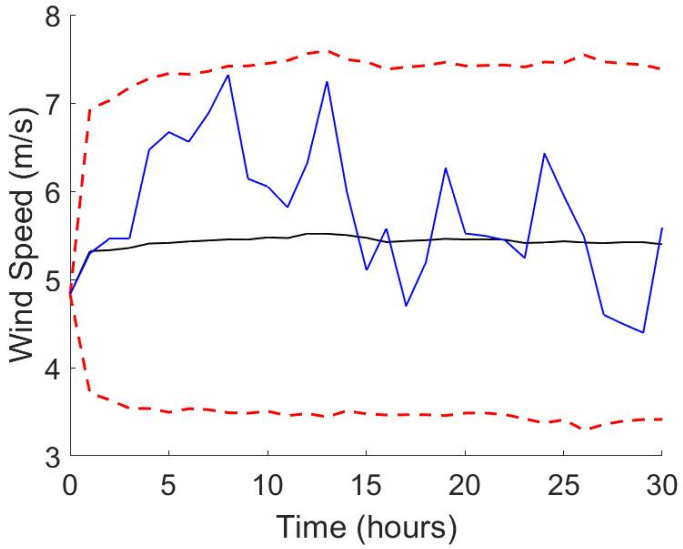

(b) MC wind speed forecast simulation with hourly data points

Figure 10: MC method simulation of a 20-month ESCI and 1-month (only the first 30 hours are shown for clarity) wind speed forecast predictions, for $N_{MC} = 1000$, are shown in Figures 10a and 10b respectively. The red dotted line, black solid line and blue solid line represent the 95% confidence intervals, mean and a sample of the forecast prediction respectively.

It is important to note the different timescales of the environmental inputs. The digital twin model projects the ESCI separate to the remainder of the model and uses it for predictions on energy sale prices. Typically, the timescales of such predictions are in the order of months [24]. Therefore, the model projects the ESCI in a discrete monthly timescale fashion, where each value is the monthly average. In contrast, the wind speed model typically has a timescale of minutes or hours and is projected forward in an hourly discrete timescale fashion, where each value is the

hourly average. Furthermore, the confidence intervals in Figure 10b remain relatively consistent as the prediction moves forward in time. However, this is not the case for the ESCI model's prediction as the confidence intervals in Figure 10a increase as the prediction moves forward in time. This finding was expected given that both of the model's element of randomness is taken from the input data distributions in Figures 5b and 6b. Where the former distribution is less prone to generate values far from its mean due to the Weibull's inability to approximate long-term wind speed trends. For industry-standard accurate wind speed prediction software, one would expect to see compensation for the unlikely event of substantial surges and declines in wind speed. This would see predictions gain a more gradual increase in confidence interval size as time propagates forward, in turn better capturing the unpredictable nature of the wind.

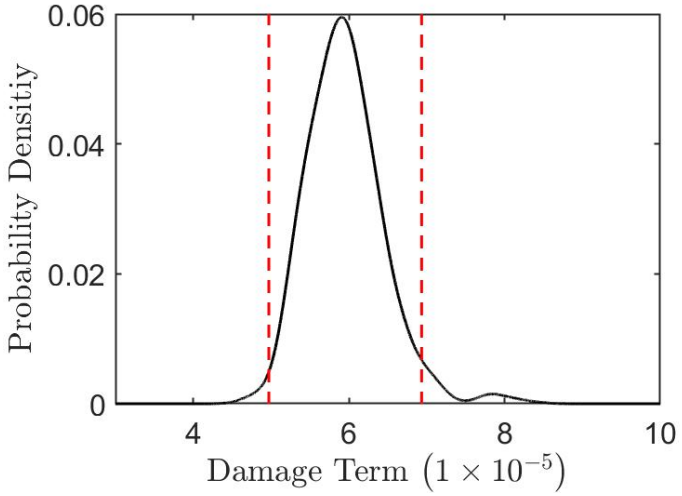

(a) MC turbine tower damage indicator, D

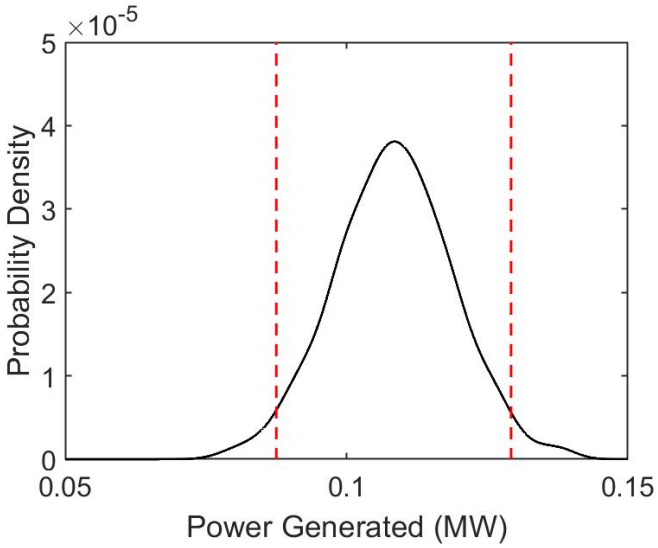

(b) MC simulation of the power projection, P (kW)

Figure 11: MC simulation of the turbine tower damage indicator, D, (11a) and average power generated (11b) subject to a MC 1-month wind speed forecast prediction (10b) with $N_{MC} = 1000$. Where the red dotted and black solid line represent 95% confidence intervals and the distribution of the resulting value respectively.

5.2 Uncertainty Management

This subsection describes how quantified uncertainties are combined in the calculations of model 3.7 presented in Figure 3. A specific investigation into how such uncertainties couple to evaluate the main deliverable of the digital twin, namely the wind turbine profit projection is explored. To begin, more assumptions are introduced separately to the model assumptions detailed in Section 3.1. The assumptions introduced here are established in order for indicative parameter values to be used in place of precise data. Thus, returning profit estimations which are used for quantitative comparisons in operational decision making. Again, it is emphasised that in practice, substantial systematic testing or the utilisation of 'digital sensors' to estimate key data and parameter values introduced in this subsection is highly advised.

Consequently, an indicative value for the wind turbine operation and maintenance (O&M) cost is explored. Manwell et al. [21] outlined how a study on a Californian wind farm concluded that the average O&M cost per kilowatt-hour ranged between 0.008 to 0.012 \$/kWh. Whereas, the International Renewable Energy Agency (IRENA) proposes statistics that infer that the actual range is between 0.013 and 0.02 \$/kWh [2]. At the time of writing this thesis, the conversion rate equates \$1 to £0.825. As a result, the range proposed by the IRENA is equivalent to 0.011-0.016 £/kWh. The IRENA also explain that robust data for wind farm O&M costs is yet to emerge [2]. Therefore, obtaining precise values would require rigorous testing specific to each wind turbine/farm. Adopting the range proposed by the IRENA as an indicative parameter value and assuming the value follows a normal distribution with mean 0.0135 £/kWh and variance 1.25×10^{-5} £/kWh, the profile of the turbine O&M cost is captured and presented in Figure 12a.

The final additional assumption is introduced in order to understand and quantify the relationship between the damage indicator and the projected O&M cost. Significantly, as the material fatigue accumulates, maintenance will need to be conducted more frequently as smaller increments are more damaging at higher values of the damage indicator. Therefore, a vital assumption is formulated to simply connect the O&M cost to the turbine tower damage indicator. It is assumed that the damage indicator in Figure 11a, simulated using the standard model parameters listed in Table 2, has a turbine O&M cost equal to that proposed by the IRENA and presented in Figure 12a. To clarify, a damage indicator with mean and variance equal to 5.95×10^{-5} and 4.91×10^{-6}, respectively, has an O&M cost with mean and variance equal to 0.0135 £/kWh and 3.502×10^{-5} £/kWh respectively.

Furthermore, it is assumed that the scaling between the corresponding values is linear. That is, a 2-fold increase in the damage indicator results in an identical 2-fold increase in the O&M cost. As a result, a scaling parameter, s, is introduced to evaluate the magnitude of the scale in the damage indicator and the resulting O&M cost, which is simply the particular simulation damage indicator divided by the indicative value 5.95×10^{-5}. For example, a damage indicator with mean 5.95×10^{-4} and variance 4.91×10^{-5} has an s value of 10, resulting in an O&M cost with mean 0.135 £/kWh and variance 0.035 £/kWh.

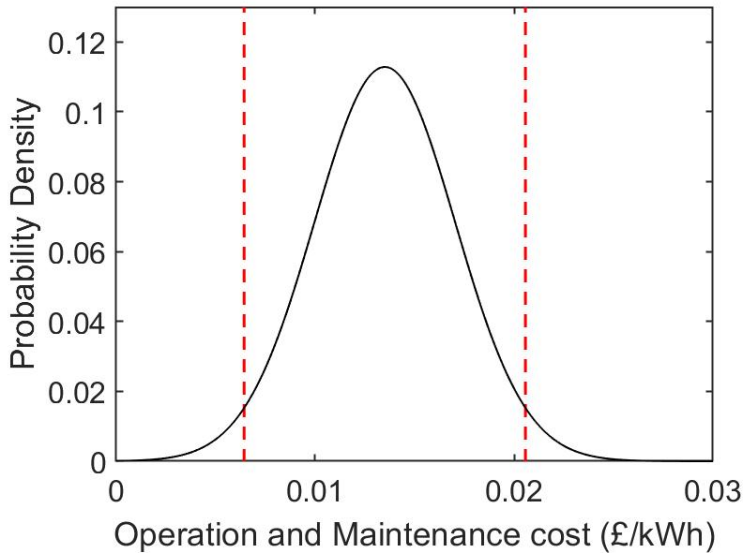

(a) O&M cost (£/kWh)

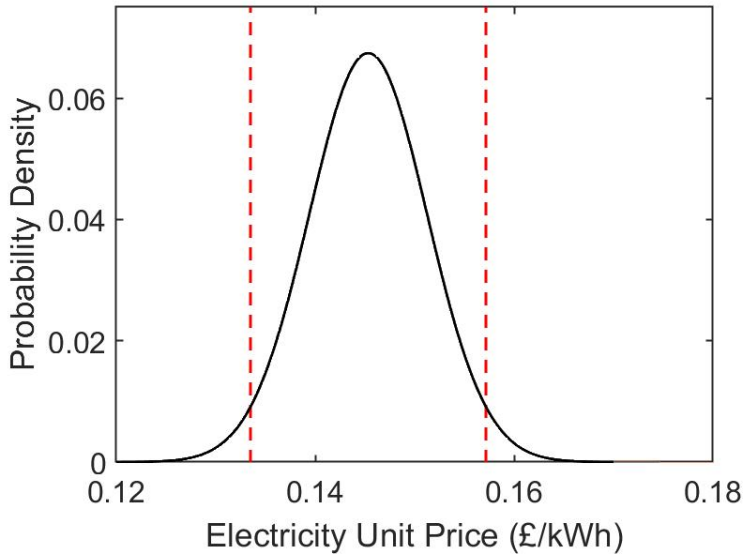

(b) Electricity supplier unit price, U_{ep} (£/kWh)

Figure 12: Normal distribution for the O&M cost and electricity supplier unit price per kilowatt-hour of energy generated (£/kWh) shown in Figures 12a and 12b, respectively. Where the red dotted and black solid line represent 95% confidence intervals and the distribution of the resulting value respectively.

Combining the wind turbine power projection, P, electricity supplier unit price, U_{ep}, and ESCI forecast following (16), the wind turbine income distribution and 95% confidence intervals can be generated. Given that the variables being concatenated are governed by specific distributions, in order to generate a resulting distribution for the wind turbine's projected income, PI, the MC method is applied again. A RN from the power and electricity supplier unit price distributions in Figures 11b and 12b respectively, were generated and multiplied to evaluate the projected income following (16). This process is simulated in an iterative scheme for a given number of

samples, N_{MC}, and the resulting distribution for PI is generated.

Given that the wind speed forecast prediction in Figure 10b is a single month in length, e_j is incorporated by simply adopting the first value in the monthly discrete ESCI forecast. If the digital twin were simulated with a longer wind speed forecast, spanning over multiple months, the PI distribution would be calculated for each respective month individually and then averaged. Simulating for the same number of samples, $N_{MC} = 1000$, a RN from the P and U_{ep} distributions are generated and multiplied following (16),

$$PI = \frac{113.54}{100} \times R_{U_{ep}} \times R_p, \tag{20}$$

where $R_{U_{ep}}$ and R_p are the randomly distributed numbers from the distributions in Figures 12b and 11b, respectively. Figure 13a presents the distribution generated following the MC simulation of Equation (20).

Identical to the method used to evaluate the distribution of the turbine projected income, PI, the MC method is utilised to estimate the turbine's projected profit, PP. The MC method is applied by generating a RN from the O&M cost, power generated and the projected income distributions in Figures 12a, 11b and 13a, respectively. Furthermore, a RN from the damage indicator distribution is generated and the resulting s value for that sample is evaluated. The RNs for each sample are used to evaluate the projected profit following (17) and the procedure is iterated for all N_{MC} samples in order to generate the resulting distribution. Simulating for $N_{MC} = 1000$ samples, the iterative procedure is governed by

$$PP = R_{PI} - s(R_P \times R_{O\&M}), \tag{21}$$

where R_{PI} and $R_{O\&M}$ are the randomly distributed numbers from the distributions in Figures 12b and 11b, respectively. Figure 13b presents the distribution for the projected profit, PP, for MC simulations following (21) with an s value of 1 (black) and 150 (blue).

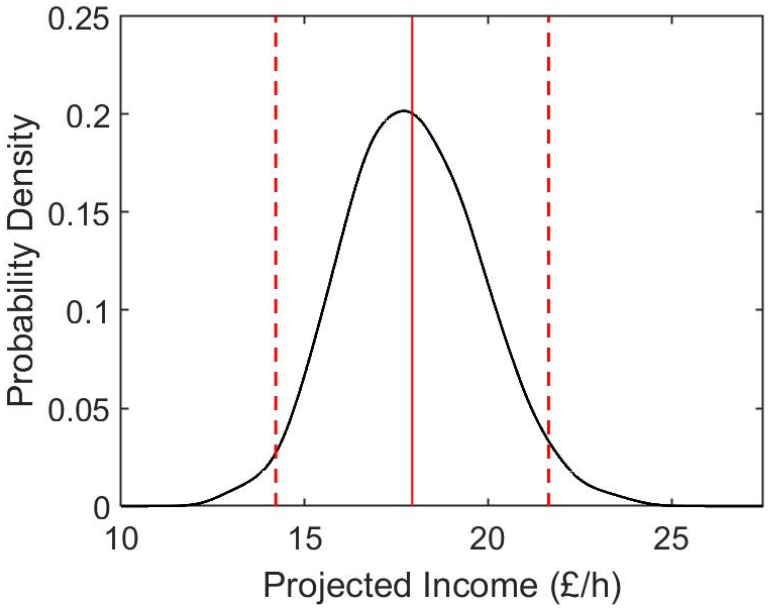

(a) MC projected income, PI (£/h)

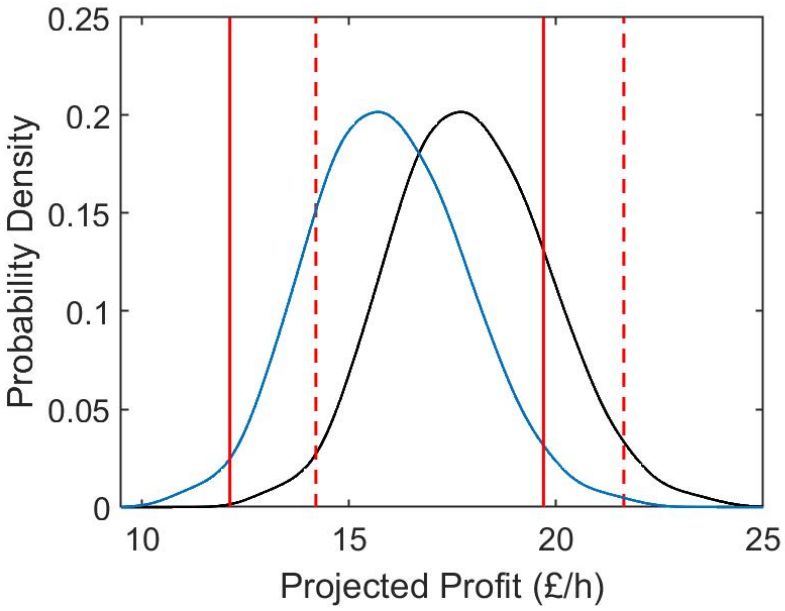

(b) MC projected profit, PP (£/h)

Figure 13: Resulting distributions for the MC simulations of the wind turbine projected income, shown in Figure 13a, and profit shown in Figure 13b. Figure 13b presents black and blue distributions that have an s value of 1 and 150, respectively. Furthermore, the dotted red lines and solid red lines represent the 95% confidence intervals of the black and blue distributions respectively.

6 Operational Decisions

As outlined in Section 1.2, the digital twin model aims to manage and propagate uncertainties, providing the ability to pre-set informed operational decisions in real-time for predicted forecasts. This section specifically analyses the operational decision of pre-setting a wind turbine cut-out wind speed for an upcoming wind speed and ESCI forecast. As explained in Section 3.1, the turbine cut-out wind speed governs the conditions whereby the turbine is scheduled to shut down. Therefore, adjusting this variable directly affects both the power generated and damage accumulated. Optimising this variable and pre-setting it for the upcoming forecasts can minimise O&M costs while maximising the power extracted. Consistently doing so, especially during high wind speed forecasts that see repercussions to damage accumulation, crucial long-term improvements to profit can be sustained. To experiment with this variable, four wind speed, (μ_v, σ_v), and three ESCI, (μ_e, σ_e), extreme monthly-long scenarios are combined. Simulating for these extremes, the maximum projected profit is optimised for the future scenario and the resulting wind turbine cut-out wind speed is returned.

In order to optimise the wind turbine cut-out wind speed in such a way, a range of cut-out values is passed to the framework presented in Figure 3. These values are incorporated into the components of the framework where the 'Wind Turbine Characteristics' inputs are labelled. For the respective cut-out value, the model components are simulated, and a cut-out specific projected profit is returned. Once the digital twin has been simulated for each of the respective wind turbine cut-out values, the maximum projected profit value is evaluated using the *max* MATLAB function and listed in Table 5a. This maximum value is cross-referenced back to the range of cut-out values, and the value specific to the maximum profit is identified and listed in Table 5b.

(μ_e, σ_e) \ (μ_v, σ_v)	Gale (24.02,3.20)	High (16.08,1.24)	Medium (8.04,0.87)	Low (5.36,0.71)
High (128.4,10.0)	-150.60	465.30	87.74	22.50
Medium (102.8,8.0)	-389.80	363.51	70.23	17.60
Low (82.2,6.4)	-412.86	285.10	56.20	14.38

(a) Maximum projected profit (£/h)

(μ_e, σ_e) \ (μ_v, σ_v)	Gale (24.02,3.20)	High (16.08,1.24)	Medium (8.04,0.87)	Low (5.36,0.71)
High (128.4,10.0)	28.02	20.34	12.80	9.25
Medium (102.8,8.0)	29.54	21.34	17.73	7.30
Low (82.2,6.4)	29.08	21.34	18.07	12.80

(b) Optimal cut-out wind speed (ms^{-1})

Table 5: Maximum projected profit (£/h) and optimal cut-out wind speed (ms^{-1}) for different combined monthly-long extreme wind speed, (μ_v, σ_v), and ESCI forecasts, (μ_e, σ_e), shown in Tables 5a and 5b respectively. The wind speed extremes include Gale, High, Medium, and Low scaled forecasts, whereas the ESCI extremes include High, Medium and Low forecasts.

Figure 14 outlines a subset of the low-medium (wind speed and ESCI forecast scenario) simulation cut-out wind speed specific profit figures with the model input uncertainties quantified. From this range of cut-out values, the optimal solution is selected and presented in Table 5 based on which profit distribution has the highest mean value.

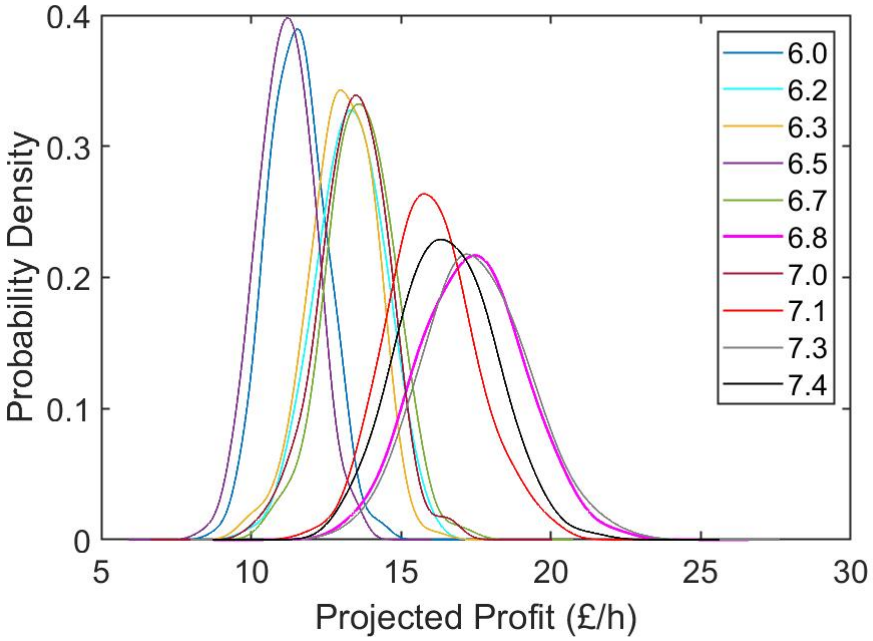

Figure 14: A subset of the resulting projected profit distributions from the simulation cut-out values for the combined medium ESCI and low wind speed scenario. The maximum mean projected profit is 17.60 £/h (grey distribution) and the resulting optimal cut-out wind speed is 7.30 ms^{-1} as shown in Tables 5a and 5b, respectively.

The results in Table 5 are heavily reliant on the model assumptions, specifically the assumptions introduced in Section 5. As a result, any analysis conducted is only relevant to the specific fidelity outlined in the assumptions and may not have an accurate connection to the real-world. However, for the particular wind turbine configuration analysed, a wind speed environment with a mean of approximately 16.08 ms^{-1} surges the model profit projections. Whereas, the energy price merely scales the projected profit. Interestingly, it is apparent that a higher electricity price lowers the optimal cut-out wind speed. This means that preserving the turbine at any given opportunity seems to increase the profit projection via savings on O&M costs.

Furthermore, the results in Table 5b imply the importance of selecting the turbine tower structure by taking surrounding environments into consideration. Operating for the course of a year in an optimal high-high environment using the optimal cut-out wind speed, the individual wind turbine projects a profit of £4,076,028. However, for the low, medium and gale wind speed environments, the wind turbine seems to struggle in comparison. The gale environment even sees negative profit projection results, suggesting that the current turbine configuration is inadequate for that specific environment. Therefore, in order to profit in this harsh environment, a more durable and resilient design should be considered. Such evaluations prior to installing a wind turbine are able to indicate whether the particular design is economically viable.

7 Conclusions

This thesis has explored how a digital twin, with simple combined models, can be used for continuous forecasting to drive decision making that optimises the projected profit, with the environment uncertainty quantified. Although significant simplifications were implemented and only single DoF dynamics were analysed, the digital twin developed fulfils all three objectives listed in Section 1.2. On the contrary to the limited dynamical analysis, the combined system is comprised of a clear fidelity that is described by the set of assumptions governing the fused simplistic models. As a result, flexibility exists to extend or exchange models for more refined and accepted versions. In doing so, a more complete digital twin model that incorporates dynamics of multiple DoF can be developed. Subsequently, the model will produce results and predictions of increased accuracy, thus enhancing its suitability in industry. For instance, given a clear level of fidelity and specialised experience, the open FAST software has the potential to substitute the models outlined in Sections 3.3 and 3.4.

When considering a purely dynamical systems perspective, there remains abundant possibilities for areas of further examination. Therefore, in no means can the existing combination of simplistic models be used to analyse the operation of a fully functioning wind turbine. However, all simplifications and assumptions were established in order to fulfil the aim and objectives of the thesis. That is, to develop a key framework of combined models in order to optimise the turbine-specific cut-out wind speed with the input uncertainty quantified. To illustrate, modelling the wind turbine as a single DOF system was advantageous in simplifying the task of evaluating the system's response subject to an applied force. Thus, enabling the investigation and analysis of the system's cyclic loading. However, in reality there is a multitude of factors that inflict cyclic loading upon the wind turbine structure. For example, the turbine blade pitch controls the aerodynamic torque, which has a significant effect on the rotor thrust, causing an additional unexplored tower excitation. Analysing and incorporating a multi DoF model that accounts for all turbine excitation factors listed in [21] would significantly increase the model's level of validity.

Relative to the wider body of literature, this thesis provides a framework for propagating and managing uncertainty in a fused system. In particular, a detailed means on quantifying the uncertainty characterised by the wind speed and energy price input data in the operational decision analysis is investigated. Contrasting outputs in the model predictive analysis are compared and analysed in terms of their distribution moments, thus increasing confidence in the interpretation and conclusions established.

Furthermore, the digital twin framework grants access to the level of accuracy in such predictive analysis to the user. Given that the MC sampling method is applied, the user of the model has control over the number of MC samples, N_{MC}, which directly controls the approximation error. However, the MC method only qualitatively evaluates and propagates the uncertainty in the inputs, providing no insight into the uncertainties in inner computations involved to transform those inputs into outputs. As a result, the uncertainty in the model's validity to the applications,

parameter values and computational error all remain unaccounted for.

Such uncertainties remain fundamental in the analysis conducted in fully operational digital twin models. Therefore, in order to develop a more complete uncertainty propagation and management framework, the incorporation of such uncertainties is required. Each of R. C. Smith [28] and the EPSRC Grant Proposal [32] provide methods that are suited to resolving such issues. These include the Markov Chain Monte Carlo (although the efficiency depends on the problem nature and available information), polynomial surrogate models, global sensitivity analysis and more. Given a substantial amount of additional time, the first course of action would be to further investigate and incorporate such uncertainties using the methods mentioned.

What cannot be overlooked is that the accuracy and validity of results critically relies on the input data provided. In order to obtain exceptionally accurate results for a particular scenario, operators of the digital twin model require access to trustworthy turbine-specific material, stochastic environment and O&M cost data. Access to precise turbine-dependent data was unavailable in the investigations outlined in this thesis. Thus, the analysis outlined is based on indicative data taken from online sources and presented in Section 4.2. Although, as suggested in various published literature [30] [32] [25], a more elegant approach would look at installing a feedback control system in the digital twin model, which fine-tunes the model parameters and predictions to specifically match that measured from the asset itself. Updating and correcting individual model predictions systematically in such a way is able to relax the user requirement for precise turbine-dependent data.

Provided feedback controller systems are fitted as early as the installation of the turbine, the model accuracy is projected to improve significantly. Thus, leading to the more efficient operation of the asset. Such systems tie in with the third, unexplored, validation model stage in creating robustly validated digital twin models as implied in the EPSRC Grant Proposal [32]. Specifically, the proposal suggests a 'traditional' approach to the verification and validation of the model, through metrics based on comparisons between model prediction and observed structural behaviour. For example, given that forecasted environments correlate with those similar to that previously experienced by the wind turbine, the projected response and power can be validated by those observed previously via metrics. Utilising incorporated feedback controller systems, such adjustments can then be fed back and implemented into the system to update the resulting projections, leading to more accurate output-analysis. With an adequate addition to the project timeframe, the framework will be extended to incorporate a validation model with the ability to generate such metrics that indicate the level of trust placed in the model predictions. This extension will reduce the disparity between the current and industry-standard robustly validating digital twin models.

Finally, the results and analysis of the developed model significantly indicate the benefits of implementing digital twin models in the design stage of the individual assets, in a multitude of areas. Sections 4.2 and 6 outlines how turbine location, material and structure design can drastically affect the performance regarding projected profit values. Whereas, the digital twin provides a framework to test different wind turbine configurations with varying environments.

Thus, providing the user with tools to optimise a set of possible installation locations, component material and structure orientation. An optimal combination of these factors, achieved by optimising such tools in conjunction with the turbine operational decisions, will allow consistent high-profit values to be sustained.

9 References

[1] S. Adhikaria and S. Bhattacharya. "Dynamic Analysis of Wind Turbine Towers on Flexible Foundations". In: *Shock and Vibration* 19 (Jan. 2012), pp. 37–56. DOI: 10.1155/2012/408493.

[2] IRENA - International Renewable Energy Agency. "Renewable Energy Technologies: Cost Analysis Series". In: 1: Power Sector (2012). URL: https://www.irena.org/Publications.

[3] H. Aksoy, Z. Toprak, A. Aytek, and N. Erdem. "Stochastic generation of hourly mean wind speed data". In: *Renewable Energy* 29.14 (Nov. 2004), pp. 2111–2131. DOI: 10.1016/j.renene.2004.03.011.

[4] O. Anaya-Lara, N. Jenkins, and J. Ekanayake. *Wind Energy Generation: Modelling and Control*. 1st ed. John Wiley Sons, Aug. 2009. ISBN: 9780470748237.

[5] Z. Botev. *Kernel Density Estimator*. Accessed: 26/02/20. MATLAB Central File Exchange, Dec. 2015. URL: https://www.mathworks.com/matlabcentral/fileexchange/14034-kernel-density-estimator.

[6] A. Cambell, J. Hanania, B. Heffernan, J. Jenden, E. Lloyd, and J. Donev. *Energy Education - Wind Power*. Accessed: 26/2/20. Sept. 2019. URL: https://energyeducation.ca/encyclopedia/Wind_power.

[7] B. Dagli, Y. Tuskan, and Ü. Gökkuş. "Evaluation of Offshore Wind Turbine Tower Dynamics with Numerical Analysis". In: *Advances in Civil Engineering* (Apr. 2018). DOI: 10.1155/2018/3054851.

[8] J. L. Devore. *Probability and Statistics for Engineering and the Sciences*. 8th ed. Cengage Learning, Dec. 2010. ISBN: 9780538733526.

[9] DNV.GL. *WindGEMINI Digital Twin for Wind Turbine Operations*. Accessed: 14/11/19. URL: https://www.dnvgl.com/services/windgemini-digital-twin-for-wind-turbine-operations-102853.

[10] Mathworks Documentation. *Estimate Coefficients of ODEs to Fit Given Solution*. Accessed: 21/11/19. URL: https://uk.mathworks.com/help/ident/ug/estimating-coefficients-of-odes-to-fit-given-solution.html.

[11] S. Evans, C. Savian, A. Burns, and C. Cooper. "Digital Twins for the Built Environment". In: *The Institution of Engineering and Technology* (Oct. 2019). Accessed: 16/11/19. URL: theiet.org/built-environment.

[12] E. F. Fama. "Random Walks in Stock Market Prices". In: *Financial Analysts Journal* 51 (1 Jan. 2019), pp. 75–80. DOI: 10.2469/faj.v51.n1.1861.

[13] R. Gallagher and A. C. Elmore. "Monte Carlo Simulations of Wind Speed Data". In: *Wind Engineering* 33 (Dec. 2009), pp. 661–674. DOI: 10.1260/0309-524X.33.6.661.

[14] C. Gavriluta, S. Spataru, I. Mosincat, C. Citro, I. Candela, and P. Rodriguez. "Complete Methodology on Generating Realistic Wind Speed Profiles Based on Measurements". In: vol. 1. 10. Apr. 2012. DOI: 10.24084/repqj10.828.

[15] GOV.uk. "Digest of UK Energy Statistics (DUKES): renewable sources of energy". In: (July 2019). Accessed: 03/03/20. URL: https://www.gov.uk/government/statistics/renewable-sources-of-energy-chapter-6-digest-of-united-kingdom-energy-statistics-dukes.

[16] Halleyhit. *Generate Random Numbers According to PDF or CDF*. Accessed: 26/02/20. MATLAB Central File Exchange, Aug. 2018. URL: https://www.mathworks.com/matlabcentral/fileexchange/68492-generate-random-numbers-according-to-pdf-or-cdf.

[17] D. J. Inman. *Engineering Vibrations*. 4th ed. Pearson, Mar. 2013. ISBN: 9780132871693.

[18] A. R. Jha. *Wind Turbine Technology*. 1st ed. CRC Press LLC, Aug. 2010. ISBN: 9781439815076.

[19] J. Jonkman. *NWTC Information Portal (FAST)*. Accessed: 23/11/19. Apr. 2018. URL: https://nwtc.nrel.gov/FAST.

[20] J. Layton. "How Wind Power Works". In: *HowStuffWorks.com* (Aug. 2006). Accessed: 04/03/20. URL: https://science.howstuffworks.com/environmental/green-science/wind-power2.htm.

[21] J. F. Manwell, J. G. McGowan, and A. L. Rogers. *Wind Energy Explained : Theory, Design and Application*. 2nd ed. Wiley, Sept. 2010. ISBN: 9780470686287.

[22] J. Masoliver, M. Montero, and G. H. Weiss. "Continuous-time Random-walk Model for Financial Distributions". In: *Physical review. E, Statistical, nonlinear, and soft matter physics* 67 (2 Feb. 2003), p. 021112. DOI: 10.1103/PhysRevE.67.021112.

[23] J. P. Murcia, P-E. Réthoré, N. Dimitrov, A. Natarajan, J. D. Sørensen, P. Graf, and T. Kim. "Uncertainty Propagation Through an Aeroelastic Wind Turbine Model Using Polynomial Surrogates". In: *Renewable Energy* 119 (Apr. 2018), pp. 910–922. DOI: 10.1016/j.renene.2017.07.070.

[24] Ofgem. *Supplier Cost Index - Previous Updates*. Accessed: 23/2/20. Feb. 2018. URL: https://www.ofgem.gov.uk/publications-and-updates/supplier-cost-index-previous-updates.

[25] D. Pomerantz. *The French Connection: Digital Twins From Paris Will Protect Wind Turbines Against Battering North Atlantic Gales*. Apr. 2018. URL: https://www.ge.com/reports/french-connection-digital-twins-paris-will-protect-wind-turbines-battering-north-atlantic-gales/.

[26] Duchamp S. *GE Announces Haliade-X, the World's Most Powerful Offshore Wind Turbine*. Accessed: 04/03/20. Mar. 2018. URL: https://www.genewsroom.com/press-releases/ge-announces-haliade-x-worlds-most-powerful-offshore-wind-turbine.

[27] J. Schijve. *Fatigue of Structures and Materials*. 2nd ed. New York: Springer, 2009. ISBN: 9781402068072.

[28] R. C. Smith. *Uncertainty Quantification: Theory, Implementation, and Applications*. Philadelphia: Society for Industrial and Applied Mathematics, Mar. 2014. ISBN: 9781611973211.

[29] C. Su, Q. Jin, and Y. Fu. "Correlation Analysis for Wind Speed and Failure Rate of Wind Turbines Using Time Series Approach". In: *Journal of Renewable and Sustainable Energy* 4 (3 June 2012). DOI: 10.1063/1.4730597.

[30] A. R. Tsouroukdissian, C. E. Carcangiu, I. Pineda, T. Fischer, B. Kuhnle, M. Scheu, and M. Martin. "Wind Turbine Structural Damping Control for Tower Load Reduction". In: IMAC XXIX A Conference and Exposition on Structural Dynamics. Jan. 2011.

[31] Renewable UK. *Wind Energy*. Last accessed 14/11/19. URL: https://www.renewableuk.com/page/WindEnergy.

[32] D. Wagg, S-K. Au, J. Clarkson, S. Elliott, M. Friswell, R. Langley, S. Neild, and K. Worden. "EPSRC Grant Proposal: Digital Twins for Improved Dynamic Design". Accessed: 23/11/19. 2017.

[33] Zakeriya. *Mechanical Design in Optical Engineering*. Accessed: 24/02/20. Mar. 2013. URL: https://www.scribd.com/document/128204482/Mechanical-Design-in-Optical-Engineering.

Appendix A Central Limit Theorem

As defined by Devore [8], the Central Limit Theorem states:

Let $X_1, X_2, X_3, ..., X_n$ be a random sample from a distribution X with mean μ and variance σ^2. Then if n is sufficiently large, the sample mean, $\bar{X}$, has approximately a normal distribution with mean $\mu_{\bar{X}} = \mu$ and variance $\sigma^2_{\bar{X}} = \frac{\sigma^2}{n}$. The larger the value of n, the better approximation. In order for this theorem to hold, a Monte-Carlo sample size, N_{MC}, of greater than 30 is at least required. The accuracy of the method relies on the amount of samples used.

Appendix B 2-MW Turbine Characteristics

Characteristics of a 2-MW wind turbine that will be used in the model:

- Rated power capacity: 2 MW
- Desired wind speed: 25 mph
- Survival wind speed: 150 mph at the rotor
- Cut-in wind speed: 11 mph
- Cut-out wind speed: 35 mph
- Cone angle: 12°
- Inclination of axis: 0°
- Rotor speed: 35 rpm
- Blade diameter: 200 ft
- Blade twist angle: 11°
- Blade ground clearance: 40 ft
- Operational life-span: 30 years